



UNIVERSITY OF GHANA
LIBRARY



QL971.Ad9
bltc C.1
G371238



UNIVERSITY OF GHANA, LEGON

**WOUND HEALING IN THE HINDBRAIN
OF THE CHICK EMBRYO**

BY

KEVIN KOFI ADUTWUM-OFOSU



**THIS THESIS IS SUBMITTED
TO THE UNIVERSITY OF GHANA, LEGON
IN PARTIAL FULFILMENT OF THE REQUIREMENT
FOR THE AWARD OF M. PHIL DEGREE IN ANATOMY**

JANUARY, 2003

G-371238
QL971.Ad9
b1.c.c.1



DECLARATION



This thesis is based on work conducted by the author in the Department of Anatomy of the University of Ghana Medical School, and the Electron Microscopy Unit of the Nogouchi Memorial Institute for Medical Research in Legon, Accra.

All the work recorded in this thesis is original unless otherwise acknowledged in the text or by references.

This work has also not been submitted for any other degree in this or any other University.



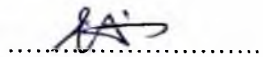
Kevin Kofi Adutwum-Ofori
(Candidate)



Prof. Aaron L. Lawson
(Supervisor)



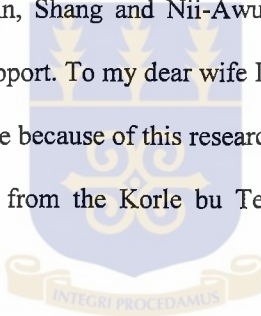
Prof. Clifford N.B. Tagoe
(Supervisor)



Dr (Mrs) Esther Dennis
(Supervisor)

ACKNOWLEDGEMENT

I give God all the glory for the grace granted me to complete this research. I am grateful to my principal supervisor, Professor A.L. Lawson, for his guidance. I wish to thank Professor C.N.B. Tagoe and Dr. (Mrs) E. Dennis, both members of the supervisory committee, for finding time to peruse and comment on this work. My gratitude also goes to Professor Fred Addai, for his useful suggestions, and Dr. Daniel Osei of the Pathology Department, for his help in acridine orange histochemistry. I do also appreciate the help of the entire staff of the Department of Anatomy of the University of Ghana Medical School, and the Electron Microscopy Unit of the Nogouchi Memorial Institute for Medical Research. I owe my colleagues (Saviour, John, Shang and Nii-Awuley) tons of thanks for their encouragement and moral support. To my dear wife I say, God richly bless you for the sacrifices you had to make because of this research. Finally, I acknowledge the financial support I received from the Korle bu Teaching Hospital through the College of Health Sciences.



DEDICATIONS

This thesis is dedicated to the Lord God Almighty, and to my wife (Yvonne) and my daughter (Nana Yaa).

LIST OF FIGURES

<u>Figure</u>	<u>Title</u>	<u>Page</u>
1a	Line drawing of a zero hour r1/r2 wound	p. 19
1b	Line drawing of a zero hour r1-r3 wound	p. 19
1c	Line drawings of transverse sections through a zero hour wound	p. 22
2a	Whole-mount of a control stage 11 embryo	p. 26
2b	Transverse LM section through the midbrain of a control stage 11 embryo	p. 27
2c	Transverse LM section through r1/r2 of a control stage 11 embryo	p. 28
2d	Transverse LM section through r3 of a control stage 11 embryo	p. 28
2e	TEM of r2 in a control stage 11 embryo	p. 29
2f	TEM of r3 in a control stage 11 embryo	p. 29
3a	Whole-mount of a control stage 12 embryo	p. 31
3b	Transverse LM section through r1/r2 of a control stage 12 embryo	p. 32
3c	Transverse LM section through r3 of a control stage 12 embryo	p. 32
4a	Whole-mount of a control stage 13 embryo	p. 34
4b	Transverse LM section through r1/r2 of a control stage 13 embryo	p. 34
5a	Whole-mount of a control stage 14 embryo	p. 36
5b	Transverse LM section through r2 of a control stage 15 embryo	p. 36
6	Transverse LM sections of a fresh r1/r2 wound	p. 39

7	Transverse LM sections of a fresh r1-r3 wound	p. 40
8	Transverse LM sections of a half hour r1/r2 wound	p. 42
9	Transverse LM sections of a half hour r1-r3 wound	p. 44
10	Transverse LM sections of a one hour r1/r2 wound	p. 46
11	Transverse LM sections of a one hour r1-r3 wound	p. 48
12	Transverse LM sections of a two hour r1/r2 wound	p. 50
13	Transverse LM sections of a two hour r1-r3 wound	p. 52
14	Transverse LM sections of twelve hour wounds	p. 54
15	Summary of the wound healing process	p. 58
16	Acridine orange whole-mount preparations	p. 60

TABLE OF CONTENTS

Declaration	i
Acknowledgement	ii
Dedications	iii
List of figures	iv
Table of contents	vi
Abstract	viii
Chapter 1 Introduction and Literature Review	1
1.1 Introduction	1
1.2 Literature review	6
1.2.1 Neural plate formation	6
1.2.2 Neural plate shaping	7
1.2.3 Neural plate bending	9
1.2.4 Neural fold formation and morphogenesis	13
1.2.5 Neural fold fusion	14
Chapter 2 Materials and methods	17
2.1 Fertilised eggs and embryos	17
2.2 Mounting of embryos	17
2.3 Wounding of embryos	18
2.4 Light microscopy and transmission electron microscopy	20
2.5 Comparison of the rates of healing of r1/r2 and r1-r3 wounds	22
2.6 Acridine orange histochemistry	23

Chapter 3. Results	. 24
3.1 Control embryos	. 24
3.2 Wound healing	. 37
3.3 Summary	. 57
3.4 Acridine orange histochemistry.	. 59
Chapter 4. Discussion	. 61
4.1 Summary of key findings	. 61
4.2 Responses of embryonic tissues to trauma	. 61
4.3 Characteristics and mechanisms of embryonic wound healing	. 63
4.4 Wound healing and morphogenesis	. 69
References	. 73
Appendix	. 87

ABSTRACT

The neural folds comprise two epithelial layers, namely, surface epithelium and neuroepithelium. In the fore and midbrain regions of the chick embryo, neural fold fusion in the dorsal midline involves a complete fusion of both layers. In the hindbrain region, however, fusion of the neuroepithelial portion of the neural folds does not occur. Rather, following apposition of the tips of the neural folds, many of the neuroepithelial cells that should participate in neural fold fusion undergo apoptosis. The rest of the neuroepithelial cells in the region of the dorsal midline undergo rearrangement and flattening to form a single-layered neuroepithelium of the hindbrain roof plate. It is not clear whether in the light of the above the hindbrain region may be a weakened portion of the neuraxis, and therefore, be predisposed to the development of neural tube defects (NTDs). The present study had a three-fold aim, namely, i) To ascertain whether the hindbrain roof plate at the time it is undergoing apoptosis possesses the ability to close when it is reopened through wounding. ii) to determine the mechanisms by which roof plate closure is achieved in the event of it occurring despite apoptosis iii) to determine whether wound healing in the hindbrain roof plate affects its morphogenetic thinning. Chick embryos at stages 11 and 12 of development were wounded in the dorsal midline of hindbrain rhombomeres r1/r2 and r1-r3, and reincubated for varying periods of time to allow healing to be effected. At zero hour, the wound was slit-like or gaped slightly, with the wound edges of the surface epithelium capping that of the neuroepithelium. Healing of both the surface epithelium and the neuroepithelium began from the ends of the wound within 30 minutes of

reincubation. Healing of both layers then progressed in a zipper-like manner towards the middle portion of the wound. The sequence of healing was surface epithelium first, followed by neuroepithelium. Complete healing occurred in both r1/r2 and r1-r3 wounds, implying that the length of the wound did not affect the ability of the hindbrain roof plate to repair itself. Additionally, the longer r1-r3 wounds healed at a faster rate than the shorter r1/r2 wounds such that at any given time, the average length of wound healed for the two groups (i.e. r1/r2 and r1-r3) did not differ significantly. Acridine orange histochemistry revealed that apoptosis in the hindbrain occurred normally in the presence of wound healing leading to the normal morphogenetic thinning of the hindbrain roof plate. The implication is that the early embryo has reparative mechanisms in place to ensure that assaults to it are taken care of, thereby preventing the interference of normal morphogenesis. Healing of the neuroepithelium in the presence of massive apoptosis suggests that apoptosis may not likely predispose the hindbrain to the development of NTDs.

CHAPTER 1

INTRODUCTION AND LITERATURE REVIEW

1.1 Introduction

The central nervous system is one of the earliest organ systems to develop in vertebrate embryos. Its development is initiated by an organized movement of its precursor cells in a process known as neurulation. This ultimately results in the formation of a neural tube, the primordium of the central nervous system (Karfunkel, 1974; Jacobson 1981; Schoenwolf, 1982; 1994; Schoenwolf and Smith, 1990a). Further differentiation of the neural tube results in the formation of the main components of the central nervous system, namely, the brain and the spinal cord. Research on neurulation has been going on for over a century (Roux, 1885; Glaser, 1914; Karfunkel, 1974; Jacobson, 1981; Schoenwolf, 1982, 1994; Schoenwolf and Smith, 1990a; Lawson and England, 1998a). The main thrust of such research has been on the determination of the mechanisms involved in the process, in order to provide a basis for understanding the aetiology of neural tube defects, as well as for the prevention and treatment of the condition (Schoenwolf, 1982; 1994; Myrianthopoulos and Melnick, 1987; Schoenwolf and Smith, 1990a; Copp *et al.* 1990; Lawson and England, 1997, 1998a).

According to early researchers, neurulation commenced with the distortion of a sheet of embryonic ectodermal cells to form a flat neural plate. This was followed by the appearance of a longitudinal furrow in the middle of the plate (Glaser,

1914). The neural plate later rolled into a neural tube when its edges were raised and came into contact with each other in the dorsal midline. Subsequently, the neural tube expanded in the brain region to form bulges known as neuromeres (Roux, 1885; Jacobson, 1981). The origin of the forces that effect neurulation was the main focus of these early studies with, some researchers reporting such forces originated within the neural plate itself (His, 1874; Roux, 1885; Glaser, 1914). Roux (1885) cultured the chick neural plate and observed that the plate rolled into a tube in a normal manner. He thus concluded that the neural plate could roll into a tube even in the absence of the adjacent tissues such as the lateral ectoderm and the underlying mesoderm. In contrast, other workers (e.g. Gillette, 1944; Schroeder, 1970) held the view that the neural tube formed as a result of forces that existed outside the neural plate, and that the dorsal and medial migration of non-neural tissue played a major role in neurulation.

Detailed investigations carried out in recent years have now thrown more light on neurulation in vertebrate embryos, showing that the process occurs in two phases: primary and secondary neurulation (Schoenwolf, 1978, 1982, 1985, 1994; Schoenwolf and Delongo, 1980; Smith and Schoenwolf, 1997). Primary neurulation involves the formation of the neural plate and its subsequent transformation into a neural tube through morphogenetic movements. Secondary neurulation, on the other hand, involves the canalisation of the medullary cord, a solid mass of cells, to form a neural tube. In higher vertebrates such as birds and mammals, the neural tube is formed by both primary and secondary neurulation

(Schoenwolf, 1978, 1982, 1984, 1994; Schoenwolf and Delongo, 1980). The formation of the prospective brain and most of the prospective spinal cord occurs during primary neurulation, whereas the extreme caudal portion of the prospective spinal cord forms during the secondary neurulation. In lower classes of vertebrates however, the neural tube forms exclusively during either primary neurulation, as in amphibians and reptiles (Rugh, 1951; Schroeder, 1970; Poznanski *et al.*, 1997) or secondary neurulation, as in fishes (Ishii, 1967; Copp and Brook, 1989; Schmitz *et al.*, 1993). Primary neurulation has been studied most extensively in the avian embryo, where it occurs in four distinct but overlapping stages: (i) formation of the neural plate, (ii) shaping of the neural plate, (iii) bending of the neural plate to form a neural groove and bilateral neural folds, and (iv) fusion of the neural folds to form a neural tube (Schoenwolf, 1978, 1982, 1994; Schoenwolf and Smith, 1990a; Smith and Schoenwolf, 1997).

Briefly, at the start of primary neurulation, epiblast cells rostral to Henson's node and those flanking the cranial part of the primitive streak, undergo apico-basal (dorsoventral) thickening to form the neural plate. The neural plate when formed is relatively short anteroposteriorly and wide mediolaterally (transversely). It then undergoes shaping, during which it becomes anteroposteriorly lengthened and transversely narrowed, and span almost the entire length of the embryo (Smith and Schoenwolf, 1997). While neural plate shaping is underway, the neural plate begins to bend, resulting in the formation of a gutter-like space (neural groove) and bilateral neural folds. Each neural fold so formed is bilaminar consisting of an

outer surface epithelial layer and an inner neuroepithelial layer. Finally, the tips of the paired neural folds are brought into contact with each other in the dorsal midline of the embryo, where they adhere to each other and fuse, and the neural tube is formed.

In the fore and midbrain regions, there is complete fusion of both surface epithelial and neuroepithelial layers. Thus, in these regions the formed roof plate comprises a simple squamous surface epithelial layer overlying a pseudostratified columnar neuroepithelial layer (Bancroft and Bellairs, 1975; Silver and Kerns, 1978). Until recently, it was presumed that a similar mode of neural fold fusion occurred in the hindbrain. A study by Lawson and England (1998a) has, however, demonstrated that in the hindbrain, fusion of the neuroepithelial layers of the neural folds does not occur. Rather, once the edges of the neural folds become apposed, massive apoptosis occurs in the dorsal midline among neuroepithelial cells that should have participated in the fusion process (Lawson and England, 1998a; Lawson *et al.*, 1999). Apoptosis is a type of cell death in which the cell actively participates in its demise without invoking any inflammatory response (Gerschenson and Rotello, 1992). The process occurs spontaneously as a controlled event in healthy tissues, organs or organisms, and plays an important role in development and growth regulation (Glucksmann, 1951). It occurs in two discrete stages (Wyllie *et al.*, 1980). First the cell undergoes nuclear and cytoplasmic condensation, eventually breaking up into a number of membrane-bound fragments containing structurally intact organelles. Next, cell the fragments termed apoptotic bodies are

phagocytosized by neighbouring cells and rapidly degraded. Apoptosis in the forming hindbrain of the chick embryo plays a significant role in the morphogenetic thinning of the hindbrain roof plate (Lawson *et al.*, 1999). Here, the process is first observed at stage 10 when the edges of the hindbrain neuroepithelial layers of neural folds become apposed to each other. By stage 11 when the process becomes marked, the dorsal midline of the neuroepithelium is disorganised due to the presence of numerous rounded apoptotic cells (Lawson and England, 1998a; Lawson *et al.*, 1999). The death of these cells significantly decreases the neuroepithelial cell population in the dorsal midline. The remaining neuroepithelial cells in the region of the dorsal midline of the hindbrain then undergo rearrangement and flattening to form a single layer of cuboidal neuroepithelial cells deep to the simple squamous surface epithelial layer. The hindbrain roof plate thus appears to be a weakened part of the neural tube.

Morgagni (1769) hypothesized that the neural tube is capable of reopening after closure leading to the formation of neural tube defects (NTDs). Experimental evidence in support of this comes from a study by van Staaten *et al.*, (1993) in which chick embryos were cultured on a curved substratum, and therefore, the posterior neural tube easily reopened. Subsequent studies by Lawson and England (1996) also indicate that NTDs may occur in the midbrain region of the chick embryo from stage 18 onwards if the neural tube reopened through wounding. This is because at these stages a reopened neural tube fails to close due to a rapid brain enlargement resulting from an increase in cerebrospinal fluid pressure in the

cranial region of the developing central nervous system. It is not clear whether similarly, a reopened hindbrain neural tube is capable of closing, considering the fact that massive apoptosis occurs in this region. Indeed, Lawson *et al.*, (1999) have suggested that the hindbrain region may be predisposed to the development of NTDs on account of this.

The present study had three main objectives: i) To ascertain whether the hindbrain roof plate at the time it is undergoing apoptosis possesses the ability to close when it is reopened through wounding, ii) to determine the mechanisms by which roof plate closure is achieved in the event of it occurring despite apoptosis, iii) to determine whether wound healing in the hindbrain roof plate affects its morphogenetic thinning.

The first two objectives were investigated by observing whole-mounts and transverse sections of hindbrain neural tube wounds under the light microscope. The third objective was investigated using acridine orange histochemistry to follow the distribution of apoptosis in the hindbrain of embryos that have been wounded, and the wounds allowed to heal.

1.2 Literature review on neurulation

1.2.1 Neural plate formation

At the start of primary neurulation, epiblast cells rostral to Henson's node, and those flanking the cranial part of the primitive streak, undergo apico-basal (dorsoventral) thickening to form the neural plate. There is evidence to suggest that

neural plate thickening may be due to microtubule and microfilament induced cell elongation and apical constriction, respectively (Schoenwolf, 1982). The neural plate so formed is pseudostratified and columnar with two main neuroepithelial cell types: spindle-shaped (fusiform) and wedged-shaped (flask-like) (Schoenwolf, 1983; Schoenwolf and Smith, 1990a). Two other cell types, namely, spherical and inverted wedge-shaped, may also be present in small numbers (Schoenwolf, 1983; Schoenwolf and Smith, 1990b). The spindle-shaped cells constitute the majority of cells in the plate at this stage. However, the different types of cells are found to intermix randomly throughout the neuroepithelium (Schoenwolf and Franks, 1984; Schoenwolf, 1988).

1.2.2 Neural plate shaping

Neural plate shaping occurs shortly after neural plate formation (Schoenwolf, 1985), and is generated by cell behaviours that reside in the neuroepithelium (i.e. intrinsic factors). These include changes in neuroepithelial cell shape, position (i.e. cell-cell intercalation), and number (i.e. cell division) (Schoenwolf, 1985, 1988, 1994; Schoenwolf and Powers, 1987; Moury and Schoenwolf, 1995).

Ultrastructural studies have revealed that neuroepithelial cells contain abundant microtubules aligned parallel to the long axis of the cells (Messier, 1969; Karfunkel, 1971; Schoenwolf, 1984). These are important for neuroepithelial cell elongation. The main evidence for the role of microtubules in neural plate shaping

comes from studies in which colchicine or cold treatment was used to depolymerise them (Handel and Roth, 1971; Schoenwolf, 1985; Schoenwolf and Powers, 1987). Here, a decrease in the height of the neuroepithelial cells was observed with a corresponding increase in the width of the neuroepithelium. The re-polymerisation of microtubules in cold-treated embryos after incubation at 38°C, together with an increase in height, and a decrease in the width of the neural plate, is further evidence that microtubules indeed play an important role in altering neuroepithelial cell shape during neural plate shaping (Handel and Roth, 1971; Schoenwolf and Powers, 1987).

There is evidence that neuroepithelial cell division contributes to the lengthening of the neural plate in the chick embryo (Sausedo *et al.*, 1997). Chick neuroepithelial cells undergo an average of two to three rounds of cell division over a 24-hour period (Smith and Schoenwolf, 1987, 1988). The plane of cleavage of a dividing cell is at right angles to the orientation of its spindle fibres (Martin, 1967; Strome, 1993). In a study to examine mitotic spindle orientation in the neuroepithelium of both chick and mouse embryos during neural plate shaping, Sausedo *et al.* (1997) found that the mitotic spindles of the cells were oriented in a rostrocaudal plane. Accordingly, cleavage planes of dividing neuroepithelial cells are expected to be perpendicular to their apical surfaces. Thus, neuroepithelial cell division is not random during neural plate shaping, but preferentially oriented to place daughter cells into the length of the neural plate rather than its width. Hence, apart from causing an increase in neuroepithelial cell number and partially

accounting for the increase in volume and surface area of the neural plate, oriented cell division also contributes to the rostrocaudal extension of the neural plate.

Schoenwolf and Alvarez (1989) have shown that changes in neuroepithelial cell position also occur during neural plate shaping, due to cell rearrangements through cell-cell intercalation (interdigitation) in a transverse plane. Since neuroepithelial cells undergo two rounds of rearrangements during neurulation, cell-cell intercalation helps in neural plate narrowing mediolaterally (transversely) and concomitant extension rostrocaudally (longitudinally). Indeed, the width reduces by about half during each round of cell rearrangements, and the length correspondingly doubles (Schoenwolf, 1985).

1.2.3 Neural plate bending

In the chick, bending of the neural plate begins in the cranial region during stages 6-7, and in the spinal region during stages 8-10. The neural plate is elevated in a gradient fashion, in a manner that resembles the closing of a door hinge. The midline remains fixed, whereas the lateral aspects elevate gradually, with the most lateral (including the most medial part of the adjacent surface epithelium) elevating most. A distinct “V” shaped neural groove is therefore formed during elevation in both the cranial and spinal cord regions, being subsequently converted into a diamond-shaped groove in the cranial region and in the extreme caudal end of the spinal cord, a region called the sinus rhomboidalis (Schoenwolf, 1994). This is the result of additional bending in the dorsolateral parts of the neural plate, effected in

such a way that the tips of the neural folds are directed medially. In the rest of the spinal cord region, where this is not observed, the two lateral halves of the neural plate come into apposition with each other in the midline, as a result of neural plate elevation. Thus, a slit-like neural groove that temporarily occludes the incipient neural tube lumen is formed (Schoenwolf and Desmond, 1984).

Neural plate bending involves two main events, namely, neural plate furrowing and neural plate folding (Schoenwolf, 1982, 1994; Smith and Schoenwolf, 1997). Neural plate furrowing is the creation of longitudinal furrows at three distinct morphological loci in the neural plate, termed hinge points. These are localised regions of the neural plate where it is anchored to adjacent tissues (Schoenwolf, 1982, 1994; Schoenwolf and Franks, 1984; Smith and Schoenwolf, 1997). A single median hinge point (MHP) first forms in the midline of the neural plate (Schoenwolf, 1985; Smith and Schoenwolf, 1987; Smith, *et al.*, 1994). It spans the entire rostrocaudal length of the neuraxis, and is anchored to the prechordal plate mesoderm and notochord in the cranial and spinal cord regions. This is followed by the appearance of paired dorsolateral hinge points in the lateral regions of the neural plate. The dorsolateral hinge points (DLHPs), in contrast, are present only at certain rostrocaudal levels of the neuraxis, namely, the cranial region and the sinus rhomboidalis. They are anchored to the adjacent surface epithelium. At the hinge points, the neuroepithelial cells become wedge-shaped, resulting in localized furrowing of the neural plate. Neural plate folding involves the rotation of the neural plate about the hinge points. Folding around the MHP results in elevation of

the lateral aspects of the flat neural plate, and that around the DLHPs results in convergence of the tips of the neural folds (Schoenwolf, 1982; Colas and Schoenwolf, 2001).

The nature of the morphogenetic forces that drive neural plate bending have been under investigation for many years (reviewed by Karfunkel, 1974; Jacobson, 1981; Schoenwolf, 1982; Schoenwolf and Smith, 1990b; Smith and Schoenwolf, 1997). Currently, it is known that these forces are generated from cell behaviours that occur both within the neural plate (i.e. intrinsic) and outside the neural plate (i.e. extrinsic). Intrinsic factors are responsible for furrowing of the neural plate (Schoenwolf, 1988, 1994). Here, the alteration of the shapes of neuroepithelial cells may play a significant role. It has been shown that whereas only 25% of neuroepithelial cells in the flat neural plate are wedge-shaped, between 65% and 70% of them become wedge-shaped as the median hinge point forms (Schoenwolf and Franks, 1984; Smith and Schoenwolf, 1988; Smith, *et al.*, 1994). Furthermore, as the dorsolateral hinge points form at the cranial region and also at the sinus rhomboidalis, at least 55% of neuroepithelial cells within the dorsolateral hinge points become wedge-shaped. Neuroepithelial cells that do not participate in hinge point formation and furrowing remain mostly spindle-shaped (Schoenwolf and Franks, 1984). Also, less than 35% of the cells in parts of the neural plate where furrowing does not occur are found to be wedge-shaped at any given time (Schoenwolf and Franks, 1984). Therefore, hinge point cell wedging may provide the motive force for furrowing (Schoenwolf, 1988). Neuroepithelial cell wedging

most likely involves both apical constriction and basal expansion, with the latter predominating over the former. Apical constriction of neuroepithelial cells is mediated by the contraction of apical bands of microfilaments present in the cells (Karfunkel, 1972, 1974; Freeman, 1972). Basal cellular expansion of neuroepithelial cells, on the other hand, is mediated by the translocation of cell nuclei to the bases of the wedging cells during cell-cycle-regulated interkinetic nuclear migration (Schoenwolf and Franks, 1984; Schoenwolf and Smith, 1990b; Smith and Schoenwolf, 1987, 1988).

Extrinsic factors are responsible for folding of the neural plate, and are generated in the lateral non-neuroepithelial tissues such as the surface epithelium and its underlying mesoderm, endoderm, and extracellular matrix (Schoenwolf, 1988; Moury and Schoenwolf, 1995). It has been shown that the surface epithelium generates the major extrinsic force for neural plate folding (Alvarez and Schoenwolf, 1992; Hackett *et al.*, 1997). When only the surface epithelium is removed before neural plate folding, this process fails to occur (Hackett *et al.*, 1997). However, when the mesoderm, endoderm and associated extracellular matrix underlying the neural plate are removed, leaving the surface epithelium intact, neural plate folding occurs normally (Alvarez and Schoenwolf, 1992). Experimental evidence suggests that the surface epithelium undergoes cell flattening (Schoenwolf and Alvarez, 1991; Schoenwolf, 1994; Moury and Schoenwolf, 1995), oriented cell division (Sausedo *et al.*, 1997) and cell-cell intercalation (Schoenwolf and Sheard, 1989; Schoenwolf and Alvarez, 1991;

Alvarez and Schoenwolf, 1991) during neural plate folding. Furthermore, studies by Lawson *et al.* (2001) in which the surface epithelium adjacent to the neural plate was labelled, have conclusively demonstrated that the surface epithelial cells indeed migrate medially during neural plate bending.

1.2.4 Neural fold formation and morphogenesis

The neural folds are located at the extremes of the neural plate. Each neural fold is double-layered, consisting of an inner layer of neuroepithelium and an outer layer of surface epithelium. Neural fold formation and morphogenesis involve four key events, namely, epithelial ridging, epithelial kinking, epithelial delamination and epithelial apposition (Lawson *et al.* 2001). Epithelial ridging is the formation of a ridge at each of the prospective surface epithelial-neuroepithelial (SE-NE) junction. It is the result of an increase in the heights of the prospective neuroepithelial cells and a decrease in the heights of the prospective surface epithelial cells at the prospective SE-NE junction during neural plate shaping (Schoenwolf, 1985; Schoenwolf and Powers, 1987; Schoenwolf and Alvarez, 1991). Concomitant with the initiation of neural plate elevation, the prospective SE-NE junction undergoes epithelial kinking. This is defined as the formation of a concave curvature at the prospective SE-NE junction of each neural fold due to changes in neuroepithelial cell arrangement. The cells become expanded at their apical ends, constricted at their basal ends and aligned radially with respect to the curvature. Shortly after the onset of epithelial kinking, epithelial delamination occurs. Here, isolated extracellular spaces develop between the surface epithelial

and neuroepithelial cells at the prospective SE-NE junction, splitting the epithelium into two distinct layers. Later on, a linear interface is established between the basal surfaces of the two epithelial layers, with both groups of cells oriented perpendicularly to the interface. The linear interface extends medially as convergence of the neural folds occurs and the basal surfaces of the surface epithelial and neuroepithelial layers finally become apposed to each other. This morphogenetic event termed epithelial apposition, seems to generate forces intrinsic to each neural fold, aiding in the convergence of the folds toward the dorsal midline in the cranial portion of the neuraxis (Colas and Schoenwolf, 2001). Epithelial apposition is extensive at the forebrain level but moderate at the hindbrain level (Lawson *et al.*, 2001). At the spinal cord level, however, little epithelial apposition occurs and the neural folds do not undergo true convergence. These findings suggest the existence of a direct correlation between the degree of epithelial apposition and the degree of convergence of the neural folds.

1.2.5 Neural fold fusion

Neural fold fusion involves closure of the neural groove, and the anterior (cranial) and posterior (caudal) neuropores. As a result of neural plate bending and convergence of the neural folds, the tips of the paired neural folds are brought into contact with each other in the dorsal midline, where they adhere to each other and fuse (Portch and Barson, 1974; Geelen and Langman, 1977, 1979; Silver and Kerns, 1978; Lawson and England, 1998a). Several studies report that species variations in the pattern of neural tube closure exist among vertebrates. In mice

and rats, the neural folds fuse at several points along the neuraxis at the same time (Morris and New, 1979; Geelen and Langman, 1977, 1979; Sakai and Yamamura, 1979; Jacobson and Tam, 1982; Sakai 1989). In humans, two sites of fusion have been identified in the cervical portion of the neural folds (O'Rahilly and Gardner, 1979; Sadler, 2000). In the chick, closure of the neural groove is observed first in the midbrain by stage 8, and it progresses both cranially and caudally to involve the forebrain, hindbrain and the spinal cord (Bancroft and Bellairs, 1975; Silver and Kerns, 1978; Schoenwolf, 1983; Lawson and England, 1998a). As stated previously, the tips of the neural folds consist of an outer surface epithelial layer and an inner layer of neuroepithelium. At the time that the tips of the neural folds become apposed to each other in the dorsal midline of the embryo, the surface epithelial layers cap the neuroepithelial layers. During neural fold fusion, therefore, the surface epithelial layer of each fold fuses with that of the contralateral neural fold, and the newly formed layer delaminates from adjacent unfused neuroepithelial layer, thus contributing ultimately to the dorsal epidermis of the embryo. Similarly, the neuroepithelial layers of the neural folds fuse deep to the surface epithelium, thus closing the neural groove. Neural fold fusion is, therefore, a double fusion involving these two epithelial layers.

The specific mechanisms involved in neural fold fusion are largely unknown. The results of several studies reveal that cell surface coats provided by extracellular matrix (Sadler, 1978; Silver and Kerns, 1978; Mak, 1978; Takahashi, 1988), cellular protrusions (Bancroft and Bellairs, 1975; Silver and Kerns, 1978), and surface projections (Mak, 1978; Geelen and Langman, 1979) may be important in

fusion. After apposition of the neural folds, extracellular matrix forms thick coats on the crests of the neural folds in amphibians (Moran and Rice, 1975; Rice and Moran, 1977; Mak, 1978), birds (Silver and Kerns, 1978; Lee *et al.*, 1978), and mammals (Sadler, 1978; Geelen and Langman, 1979). They may serve as temporary adhesives, binding the leading edges of the neural folds together as fusion occurs (Takahashi, 1988). Some surface specialisations such as lamellipodia (broad and flattened cellular processes) and filopodia (long and slender cellular processes) are also seen bridging the gap between the apposed neural folds in amphibians (Mak, 1978) and mammals (Waterman, 1975, 1976; Geelen and Langman, 1979). These are believed to help cells to migrate across the gap and cause cell intermingling. Their relative scarcity in chick embryos (Silver and Kerns, 1978), however, suggests that in these embryos their role in fusion may be minimal. Formation and migration of neural crest cells might also play an active role in neural fold fusion in the chick. The neural crest cells form before neural fold fusion occurs in the chick (Anderson and Meier, 1981; Lumsden *et al.*, 1991; Lawson and England, 1998a). They are first seen sandwiched between the surface epithelial and neuroepithelial layers of the folds (Geelen and Langman, 1979; Jaskoll *et al.*, 1991; Lawson and England, 1998a), from where they move laterally. Their migration is believed to be necessary in fusion since the neural tube fails to close when the process is inhibited (Morris and New, 1979; Morris-Kay *et al.*, 1994).

CHAPTER 2

MATERIALS AND METHODS

2.1 Fertilised eggs and embryos

Two hundred Fertilised eggs from White Leghorn chickens were obtained from Afariwaa farms in Tema, Ghana. These were set in a humidified Gallenkamp economy size incubator at 38°C for between 32 - 36 hours to obtain embryos at stages 11-12 of development (Hamburger and Hamilton, 1951). The embryos were mounted and maintained for wound healing studies using the New Culture Technique (New, 1955)

2.2 Mounting of embryos

Each egg was opened by gently tapping round the shell one-third of the way down its broad end with the handle of a pair of blunt forceps, and then removing the shell above the crack with the tips of the forceps. The thick albumen and chalazion were discarded. Some of the thin albumen was poured into a container to be used later as nutrient medium, and the remainder was discarded using a sterile Pasteur pipette. The yolk with the vitelline membrane and blastoderm was poured into a wide glass bowl containing a sufficient volume of freshly prepared saline (0.9% sodium chloride solution) to cover it completely. Any thick albumen still adhering to the vitelline membrane was removed with fine forceps. A watch glass was then placed in the bowl to receive the blastoderm.

Next, the blastoderm was brought uppermost, and the vitelline membrane cut with a pair of scissors just above the equator of the yolk, away from the edge of the blastoderm. This is to avoid detachment of the blastoderm from the vitelline membrane. The cut edge of the vitelline membrane was gripped with two pairs of forceps, one in each hand, and gently peeled off the surface of the yolk. Once free, the vitelline membrane, with the blastoderm still attached, was pulled through the saline and placed on the watch glass with the blastoderm side uppermost. A glass ring was placed on the vitelline membrane to prevent it from drifting. Care was taken to ensure that the glass ring did not fall on the embryo. The watch glass with its content was transferred to a petri dish placed under a Nikon 84534 binocular dissecting microscope. Excess saline outside the ring was removed with a pipette, and the free edge of the membrane pulled over the ring until the vitelline membrane formed a fairly flat surface underneath the ring, and the embryo was centred. The redundant edge of the membrane was cut off with the pair of scissors. Any yolk present in the glass ring and under the vitelline membrane was washed off with saline till the embryo was clearly seen. The embryos were then staged according to Hamburger and Hamilton (1951). Stage 11 embryos had 12 to 14 somites while stage 12 embryos had 15 to 17 somites.

2.3 Wounding of embryos

Four groups of embryos were wounded: (i) Group A comprised 40 stage 11 embryos wounded in rhombomere r1/r2 of the hindbrain (Fig. 1a); (ii) Group B comprised 40 stage 12 embryos wounded in rhombomere r1/r2 (Fig. 1a); (iii)

Group C comprised 30 stage 11 embryos wounded in rhombomeres r1-r3 (Fig. 1b); and (iv) Group D comprised 30 stage 12 embryos wounded in rhombomeres r1-r3 (Fig. 1b).

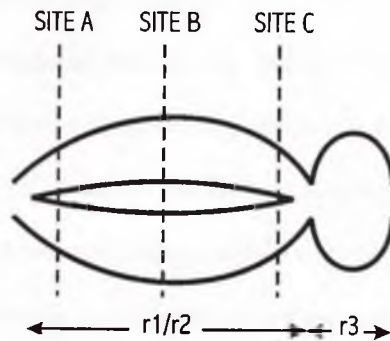


Fig. 1a. A line drawing of a whole-mount of a zero hour r1/r2 wound. The distance from site A to site C indicates the length of the wound.

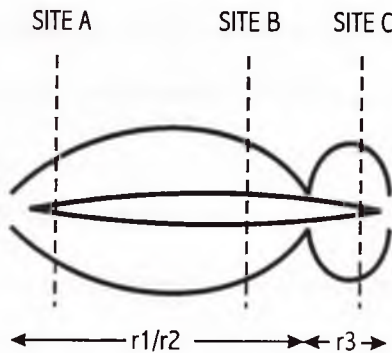


Fig. 1b. A line drawing showing a r1-r3 wound.

The glass ring was again flooded with some saline and the cranial edge of the blastoderm was carefully detached from the vitelline membrane using fine forceps (Lawson and England, 1992). The detached part was folded onto the caudal half of the blastoderm to expose the dorsal side of the neural tube. Using a sharpened and sterilised tungsten needle, a single, straight, longitudinal wound was made in the dorsal midline of the hindbrain through the surface ectoderm and the underlying neuroepithelium. The wound was carefully examined under the microscope and the observations recorded. The detached part of the blastoderm was then folded back onto the vitelline membrane and excess saline removed from the ring. The thin albumen was placed beneath the vitelline membrane, and the embryo was either processed immediately by fixation, or re-incubated for periods of between 30 minutes and 12 hours (overnight) before fixation. In the case of the latter, each wound was re-examined prior to processing. Control embryos, numbering 60, were similarly treated, except that they were not wounded. One hundred and seventy of the 200 embryos used, made up of 120 wounded and 50 control embryos, were processed for light microscopy and transmission electron microscopy.

2.4 Light microscopy (LM) and transmission electron microscopy (TEM)

Embryos used for light microscopy and transmission electron microscopy were fixed for a maximum period of 24 hours in a mixture of 2% gluteraldehyde and 2% paraformaldehyde in 0.1M sodium cacodylate buffer with calcium chloride at a final concentration of 2.5 mM and a pH of 7.2 (Martin-Partido *et al*, 1985). Next, they were washed in 0.1M sodium cacodylate buffer for an equal period of

time and post fixed with osmium tetroxide (1% in 0.1M cacodylate buffer, pH 7.2) for 30 minutes. The embryos were then dehydrated in a graded ascending series of ethanol/water mixtures up to 100% ethanol (see Appendix). They were next taken through two 30-minute changes of propylene oxide, and mixtures of propylene oxide and resin (Embed 812) in ratios of 1:1 and 1:2 respectively before being finally embedded in 100% Embed 812 using 21-well embedding moulds. The moulds, with the embedded embryos were kept for at least 48 hours in an oven set at 60°C for the resin to polymerize.

Specimens for light microscopy were trimmed with razor blades and sectioned serially at two microns (2 μ m) in a plane perpendicular to the longitudinal axis of the neural tube with a Leica Ultracut R automatic microtome. The sections were picked up serially with a pair of jeweller's forceps and transferred to drops of distilled water on clean glass slides. The slides were then placed on a hot plate set at 100°C for a few minutes to allow the drops of water to evaporate, and the sections to stick unto the slides. The sections were stained using 1% toluidine blue in 1% sodium tetraborate. Excess stain was washed off with distilled water, and after drying for about a minute, the sections were cover-slipped using DPX mountant. Next, the sections were examined at both low and high magnifications under an Olympus BHB light microscope fitted with an Olympus C-35AD camera, and pictures of the sections were taken (see Fig. 1c).

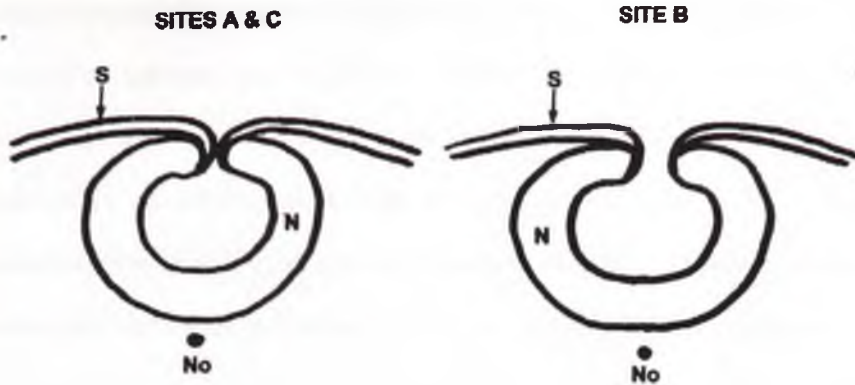


Fig. 1c. Line drawings of transverse sections through the ends (sites A and C), and the middle (site B) portions of a zero-hour wound. The wound edges are slit-like at A and C, but gape slightly at B. *S*- surface epithelium, *N*-neuroepithelium, *No*-notochord.

For TEM, the blocks were trimmed and sectioned till the midbrain-hindbrain junction was in sight. Ultra thin sections of r1/r2 and r3 of the hindbrain were then cut with a diatome diamond knife. The sections were mounted on 150-mesh copper grids dipped in 100% acetone, and stained with 2% uranyl acetate for five minutes. They were left to dry and then contrast-stained with 2% lead citrate for three minutes. The sections were later viewed with a HITACHI H-600 transmission electron microscope.

2.5 Comparison of the rates of healing of r1/r2 and r1-r3 wounds

Statistical analysis was carried out, using the student's *t* test, to compare the rates of healing of r1/2 and r1-r3 wounds. First, the length of each wound was determined by multiplying the number of sections that contained the wound by the thickness of each section (2 μ m). The mean lengths of both r1/r2 and r1-r3 wounds at the various time points (0hr, 0.5hr, 1hr and 2hrs) were calculated. From these

values the rate of healing was determined for both r1/r2 and r1-r3 wounds, and the student's *t* test was used to determine whether the differences between the two rates were significant. Additionally, the length of each wound healed at the above time points was used to calculate the percentage of the wound healed for the two groups of wounds (i.e. r1/r2 and r1-r3), and the student's *t* test was again used to determine whether the differences between the percentages were significant.

2.6 Acridine orange histochemistry

Acridine orange histochemistry was used to determine the presence and distribution of apoptosis in the hindbrain of both control and wounded embryos. Thirty embryos out of the 200 acquired were used. These were made up of 10 embryos each from groups A and B, and 10 control embryos. Five of the wounded embryos were processed as fresh wounds. They were immediately kept at 38°C for 30 minutes in phosphate buffered saline (PBS) containing acridine orange at a concentration of 5 microgrammes per milliliter (5µg/ml). The rest were incubated for thirty minutes, one hour or two hours after wounding, and later washed in PBS before re-incubating in PBS containing acridine orange. Following re-incubation, all embryos were further washed in PBS. Each embryo was then trimmed by cutting off part of the extra embryonic tissues, and mounted in 20% glycerine on a glass slide. After mounting, the embryos were immediately examined as whole mounts with a Leica MicroStar IV fluorescence microscope using a fluorescein (FITC) filter.

CHAPTER 3

RESULTS

3.1 Control embryos

3.1.1 Stage 11 embryos

Examination of control stage 11 embryos as whole mounts revealed that between 12 and 14 pairs of somites were present (Fig. 2a). Fusion of the neural folds had already occurred in the primary brain vesicles i.e. forebrain, midbrain and hindbrain. Transverse sections through the fore and midbrain neuromeres revealed that the neuroepithelium of the dorsal midline in these regions was pseudostratified columnar (see Fig. 2b). In the hindbrain, there were five neuromeres (rhombomeres), designated as r1/r2, r3, r4, r5, and r6/r7. Transverse sections through r1/r2 and r3 confirmed that there was complete fusion of the surface epithelial components of the neural folds in the dorsal midline of these rhombomeres (Figs. 2c & 2d). The fused surface epithelial layer in the dorsal midline of both r1/r2 and r3 comprised a single layer of flattened cells. In contrast, although the neuroepithelial components of the neural folds were apposed to each other in the dorsal midline of these rhombomeres, they appeared to be disorganised here when compared with the neuroepithelium of the dorsal midline of the fore and midbrains (cf. Fig. 2c with Fig. 2b). In the caudal part of r1/r2, the neuroepithelial layer in the dorsal midline had an eminence that projected into the neural tube lumen (Fig. 2c). This was absent in r3 (Fig. 2d). In spite of this difference, the cells in the dorsal midline of the neuroepithelial layer in both rhombomeres were rounded (Fig. 2c & 2d). Examination by transmission electron microscopy (TEM)

showed that these cells were undergoing apoptosis (Figs. 2e & 2f). They possessed fragmented nuclei and condensed chromatin material. Elsewhere in the neuroepithelium, the cells were mostly elongated, comprising both spindle and wedge-shaped forms. Sandwiched between the fused surface epithelium and the neuroepithelial layer in r1/r2, was a mass of cells identified as migratory neural crest cells (Fig. 2c). These were located dorsal to the basal surface of the neuroepithelial layer. These migratory neural crest cells were absent from the dorsal aspects of the basal surface of the neuroepithelium in r3 (Fig. 2d).

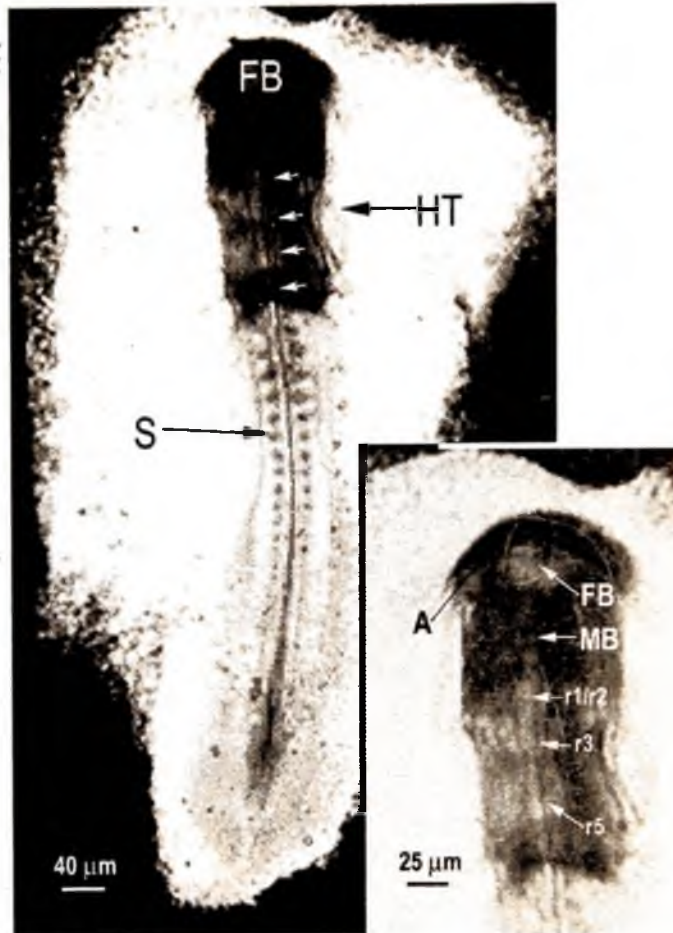


Fig. 2a. Whole-mount showing the dorsal surface of a control stage 11 embryo. The primary brain vesicles (i.e. forebrain, *FB*; midbrain, *MB*; and hindbrain, white arrows) have formed (see Inset), and the amnion (*A*) covers part of the forebrain. *HT*- heart, *r*- rhombomere, *S*- somite.

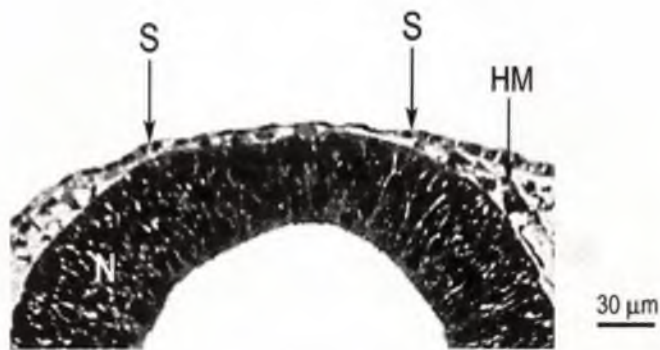


Fig. 2b Transverse LM section through the midbrain of a stage 11 control embryo. Neuroepithelium of the dorsal midline is pseudostratified columnar. *S*- surface epithelium, *N*- neuroepithelium, *HM*- head mesenchyme

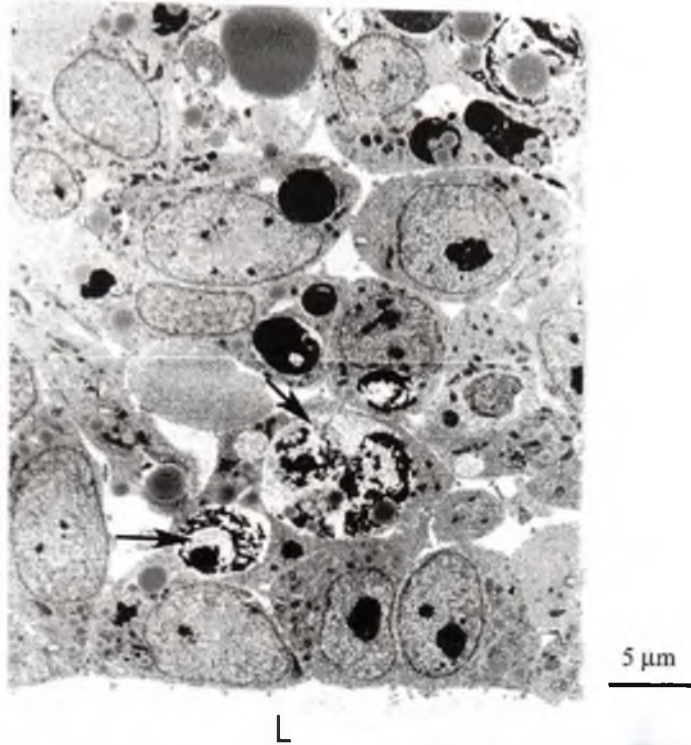


Fig. 2e. TEM of the roof plate of r1/r2 in a control stage 11 embryo showing part of the neuroepithelial eminence. There are many rounded cells, some of which are undergoing apoptosis (*Arrows*). *L*- neural tube lumen.

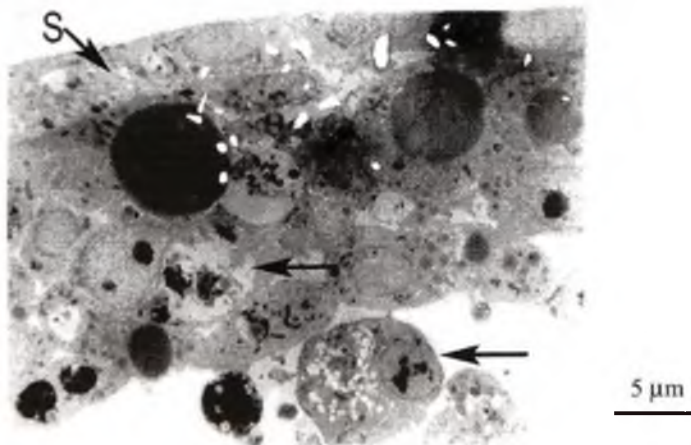


Fig. 2f. TEM of the roof plate of the dorsal midline of r3 in a control stage 11 embryo showing the surface epithelium (S) and the disorganised neuroepithelium deep to it. Arrows- apoptotic cells.

3.1.2 Stage 12 embryos

Control stage 12 embryos had between 15 and 17 pairs of somites (Fig. 3a). When examined as whole-mounts, the embryos appeared similar to those at stage 11 except that most of them were larger in size than the latter. Transverse sections through r1/r2 and r3, however, revealed some differences between stages 11 and 12 embryos. In stage 12 embryos, the dorsal midline of the apposed neuroepithelial layer seemed reduced in its full thickness in these rhombomeres (Figs. 3b and 3c). The reduction in thickness was more marked in the caudal part of r3 (Fig. 3c). Here, the reduction in thickness extended to include the dorsolateral aspects of the neuroepithelial layer. The cells in the disorganised dorsal midline of the neuroepithelial layer of r1/r2 and r3 were also fewer in number than observed at stage 11. Additionally, at stage 12, the midline neuroepithelial eminence seen in r1/r2 had significantly reduced in size in most embryos. However, migratory neural crest cells were still present between the surface epithelial and neuroepithelial layers in r1/r2.

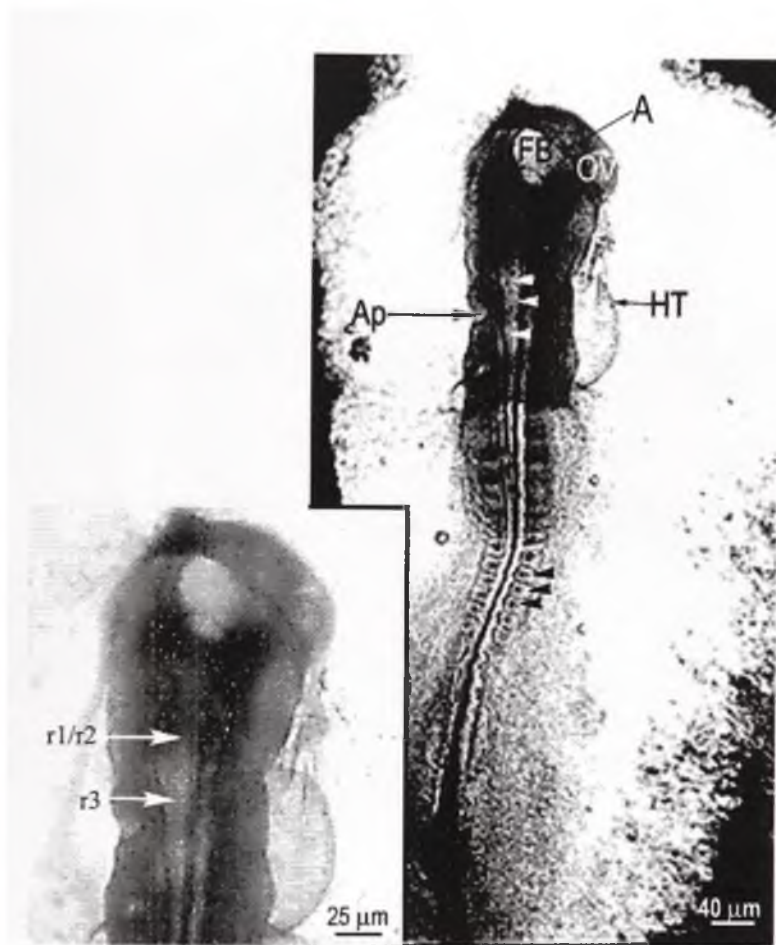


Fig. 3a. Whole-mount showing the dorsal surface of a control stage 12 embryo. *A*- amnion, *FB*- forebrain, *HT*- heart, *OV*- optic vesicle, *Ap*- Auditory pit, *White arrowheads*- hindbrain, *Black arrowheads*- somites. Inset: the cranial region magnified to show rhombomeres r1/r2 and r2 of the formed hindbrain.

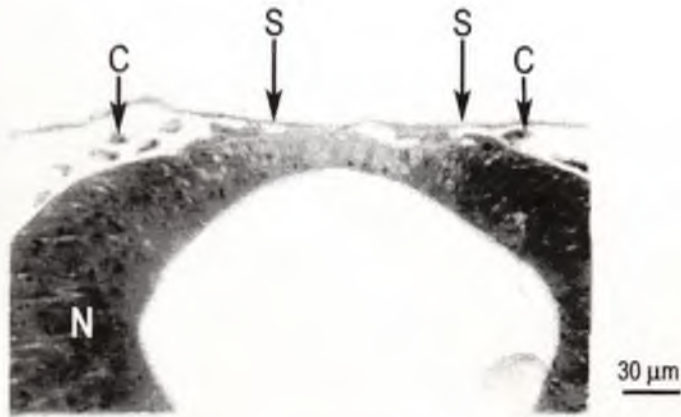


Fig. 3b. Transverse LM section through r1/r2 of a control stage 12 embryo. There is a reduction in the full thickness of the neuroepithelium in the dorsal midline, and the neuroepithelial eminence seen at stage 11 has disappeared. *S*- surface epithelium, *N*- neuroepithelium. *C*- migratory neural crest cells.

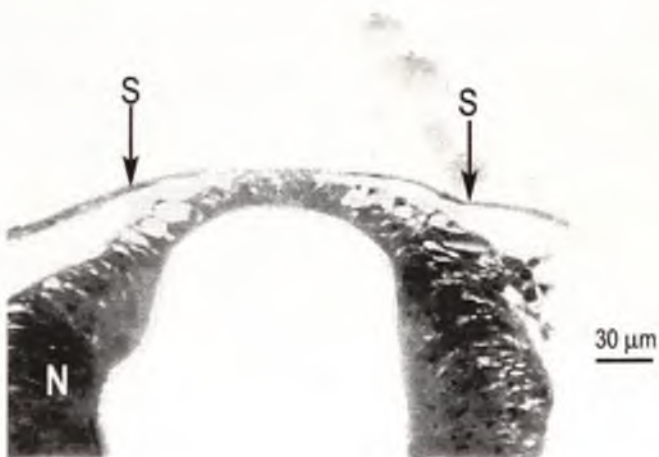


Fig. 3c. Transverse LM section through r3 of a control stage 12 embryo. As in Fig. 3b, the neuroepithelium in the dorsal midline is reduced in its full thickness, and has fewer number of cells. *S*- surface epithelium, *N*- Neuroepithelium.

3.1.3 Stage 13 embryos

When examined as whole-mounts, control stage 13 embryos had between 18 and 20 pairs of somites, and appeared larger in size than control stage 12 embryos (Fig. 4a). Transverse sections through r1/r2 and r3 showed that the full thickness of the neuroepithelial layer in the dorsal midline of these rhombomeres was significantly reduced when compared with those at stages 11 & 12 (Fig. 4b). Here, the roof plate comprised a simple squamous surface epithelium overlying a single layer of cuboidal neuroepithelial cells. Additionally, the midline neuroepithelial eminence, observed in r1/r2 at stage 11, had disappeared in all stage 13 embryos (Fig. 4b).

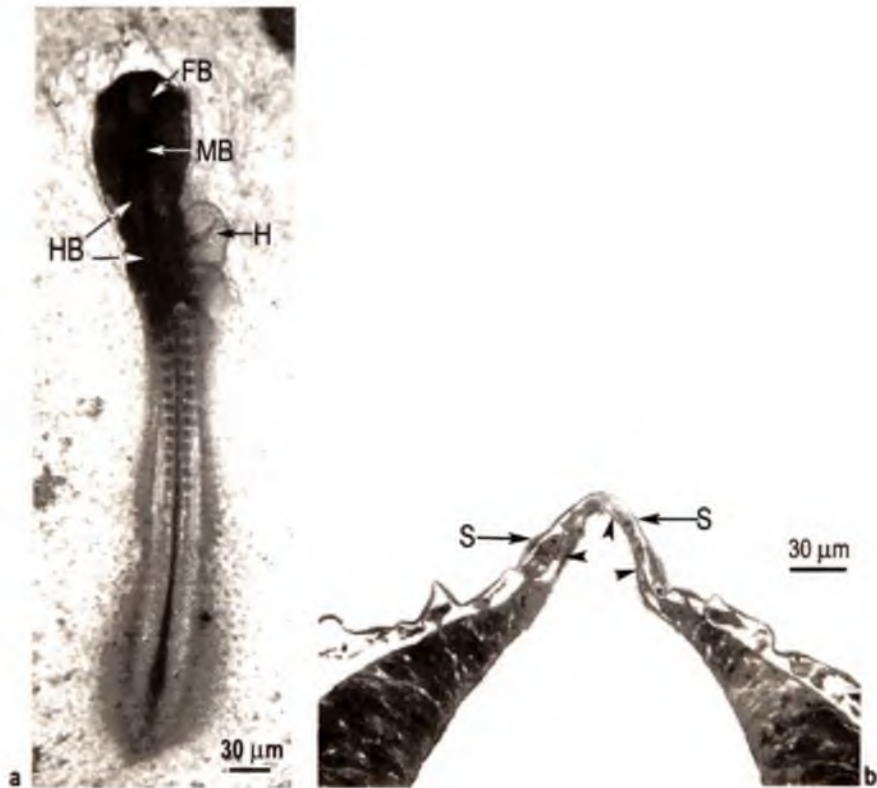


Fig. 4. (a) Whole-mount showing the dorsal surface of a control stage 13 embryo. *FB*- forebrain, *MB*- midbrain, *HB*- hindbrain, *H*- heart.

(b) Transverse LM section through r2 of a control stage 13 embryo.

Neuroepithelium of the dorsal midline comprises simple cuboidal cells (*arrowheads*). *S*- surface epithelium

3.1.4 Stages 14 and 15 embryos

Control embryos at stages 14 and 15 had 21 to 23 and 24 to 26 pairs of somites, respectively. They showed similar features, and are thus described together. In transverse sections, the roof plate of rhombomeres r1/r2 and r3 of these embryos, like that at stage 13, comprised a simple squamous surface epithelium and a simple cuboidal neuroepithelium. However, thinning of the roof plate in embryos at stages 14 and 15 extended more laterally than in stage 13 embryos (cf. Fig.5b with Fig. 4b).

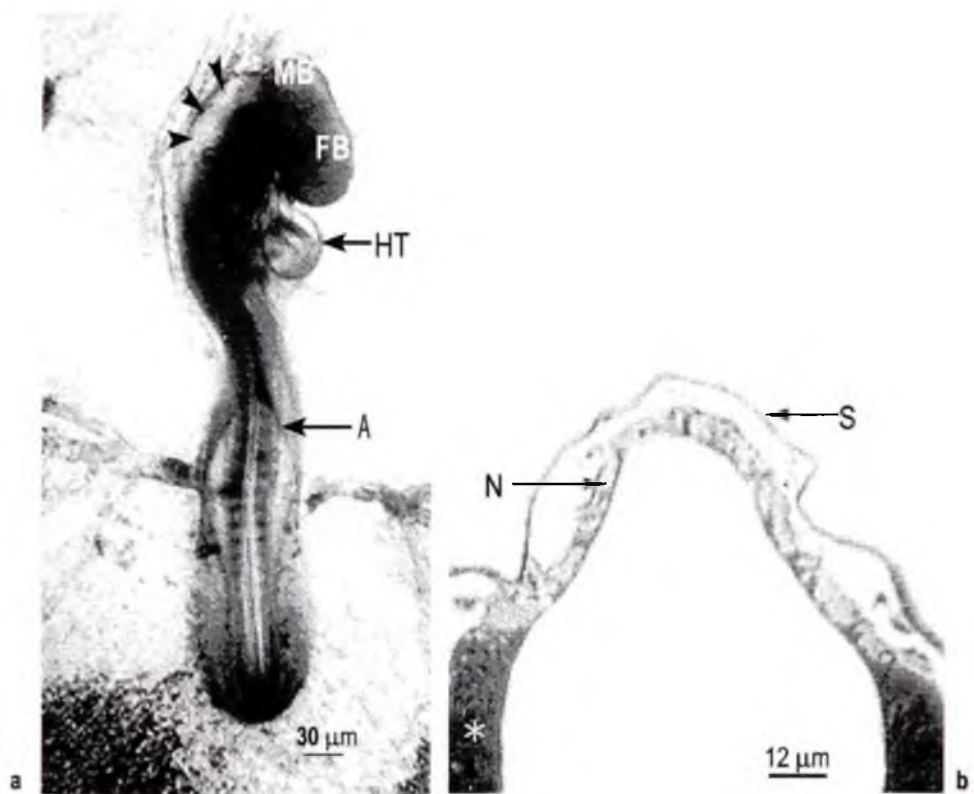


Fig. 5. (a) Whole-mount showing the dorsal surface of a control stage 14 embryo. The roof plate of the hindbrain (Arrowheads), appears translucent suggesting a reduction of its thickness. The amnion (*A*) now covers all the primary vesicles and the rostral part of the spinal region. *FB*- forebrain, *MB*-midbrain, *HT*- heart.
 (b) Transverse LM section through r2 of a control stage 15 embryo. There is extensive thinning of the roof plate. *S*- surface epithelium, *N*- dorsally-placed neuroepithelium, *Asterisk* indicates laterally-placed neuroepithelium.

3.2 Wound healing

The results indicated that the healing of neural tube wounds in stages 11 and 12 embryos followed a similar pattern. Therefore, they are described together. The wounds are described at three levels, namely, rostral (site A), middle (site B), and caudal (site C) (see Figs. 1a & 1b). The length of the wound is defined as the length along the longitudinal axis of the wound (i.e. A-C).

3.2.1 Zero hour (fresh) wounds

3.2.1.1 r1,r2

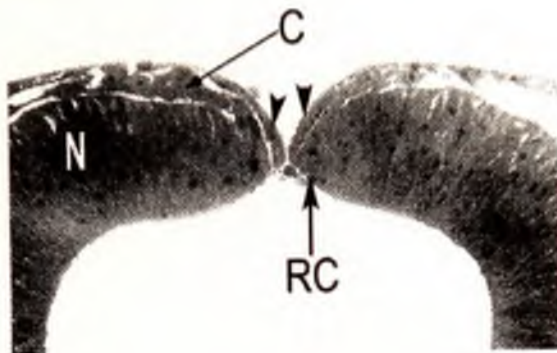
Fresh r1/r2 wounds appeared slit-like or gaped slightly when examined as whole-mounts. Examination of transverse sections of each wound revealed that it involved a full thickness of both surface epithelial and neuroepithelial layers of the roof plate. At its ends (i.e. at sites A and C), both surface epithelial and neuroepithelial wounds were slit-like (Figs. 6a & c). The edges of the surface epithelial wounds curled towards the neuroepithelium in such a manner that they capped the edges of the adjacent neuroepithelial wound (Fig. 6a). Neuroepithelial cells in the immediate vicinity of the neuroepithelial wounds were rounded; they appeared similar to neuroepithelial cells in the dorsal midline of control (unwounded) embryos (Figs. 6a & c). The morphology of both surface epithelial and neuroepithelial wounds at site B was similar to that at sites A and C except that at site B the wounds gaped slightly (Fig. 6b). The extent of gaping varied even among embryos of the same stage. In most of the embryos, the neuroepithelial eminence seen in the control embryos was split into two halves (Fig. 6c).

Migratory neural crest cells were identified between the surface epithelium and the basal surface of the neuroepithelium along the whole extent of the wound.

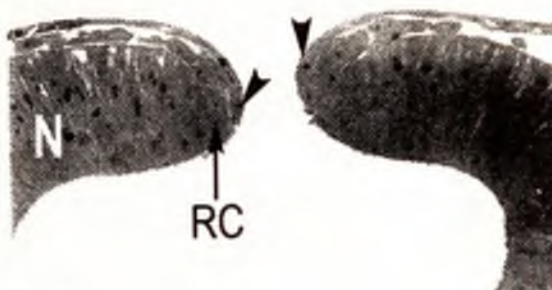
3.2.1.2 r1-r3

When examined as whole-mounts, freshly made r1-r3 wounds were longer than those involving only r1/r2, but shared similar characteristics with the latter. Transverse sections through the wounds confirmed that both surface epithelial and neuroepithelial wounds appeared slit-like at sites A and C but gaped at site B (cf. Figs. 7a-c and 6a-c). The appearance of the cells at the edges of the r1-r3 wounds was also similar to that at the edges of the r1/r2 wounds. Some migratory neural crest cells were seen sandwiched between the surface epithelial and neuroepithelial layers at sites A and B but were absent at site C, thus confirming that the wounds involved both r1/r2, where neural crest cells migrate out of the neural tube, and r3 where neural crest cells do not migrate.

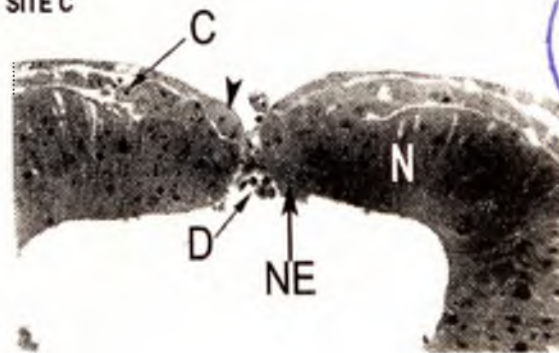
a SITE A



b SITE B



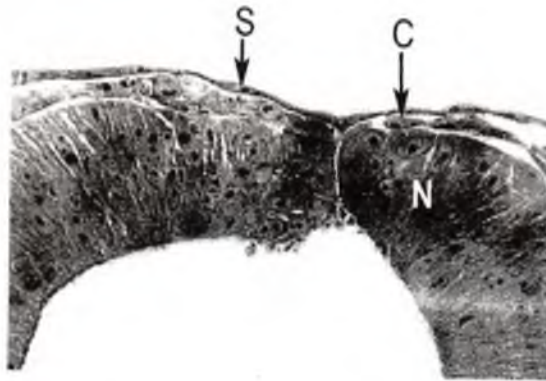
c SITE C



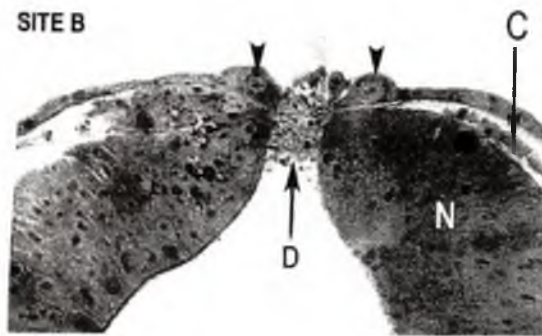
30 μm

Fig. 6. Transverse LM sections of a zero hour r1/r2 wound. Both the surface epithelial and neuroepithelial wounds are slit-like at sites A and C. In contrast, they both gape slightly at site B. The wound edges of the surface epithelium (*Arrowheads*) cap the edges of the neuroepithelium (*N*) at all three sites. *NE*- neuroepithelial eminence (divided), *C*- migratory neural crest cells, *D*- cell debris, *RC*- rounded neuroepithelial cell.

a SITE A



b SITE B



c SITE C



Fig. 7. Transverse LM sections of a zero hour r1-r3 wound. The wound edges at site B gapes slightly, with a plug of cell debris (*D*) filling the gap. *S*- surface epithelium, *Arrowheads*- rounded surface epithelial cells, *N*- neuroepithelium, *C*- migratory neural crest cells.

3.2.2 Half-hour reincubation

3.2.2.1 r1.r2

Following thirty minutes of reincubation, the wounds showed signs of healing from their ends (at sites A and C). The wound edges were in contact with each other at these sites. Here, transverse sections of the wounds revealed that the surface epithelial wound edges had fused, and therefore, the healed surface epithelium consisted of a continuous sheet of cells which curled towards the neuroepithelium, creating a “V” shaped depression (Figs. 8a & c). At site B, the surface epithelial wound edges were separated by a gap, with the cells at the wound edges capping the neuroepithelial cells as before (Fig. 8b). The gap between the wound edges appeared narrower than it was at zero hour in most embryos (cf. Fig. 8b with 6b). As in the surface epithelium, the edges of the neuroepithelial wounds were in contact with each other at sites A and C, but separated by a gap at site B (Figs. 8a, b & c). However, at all three sites, neuroepithelial cells in the immediate vicinity of the neuroepithelial wounds were still rounded. There was also no significant change in the size of the neuroepithelial eminence when compared to its size at zero hour (cf. Fig 8c with 6c), and migratory neural crest cells were sandwiched between the surface epithelium and the neuroepithelium (Fig. 8a, b & c).

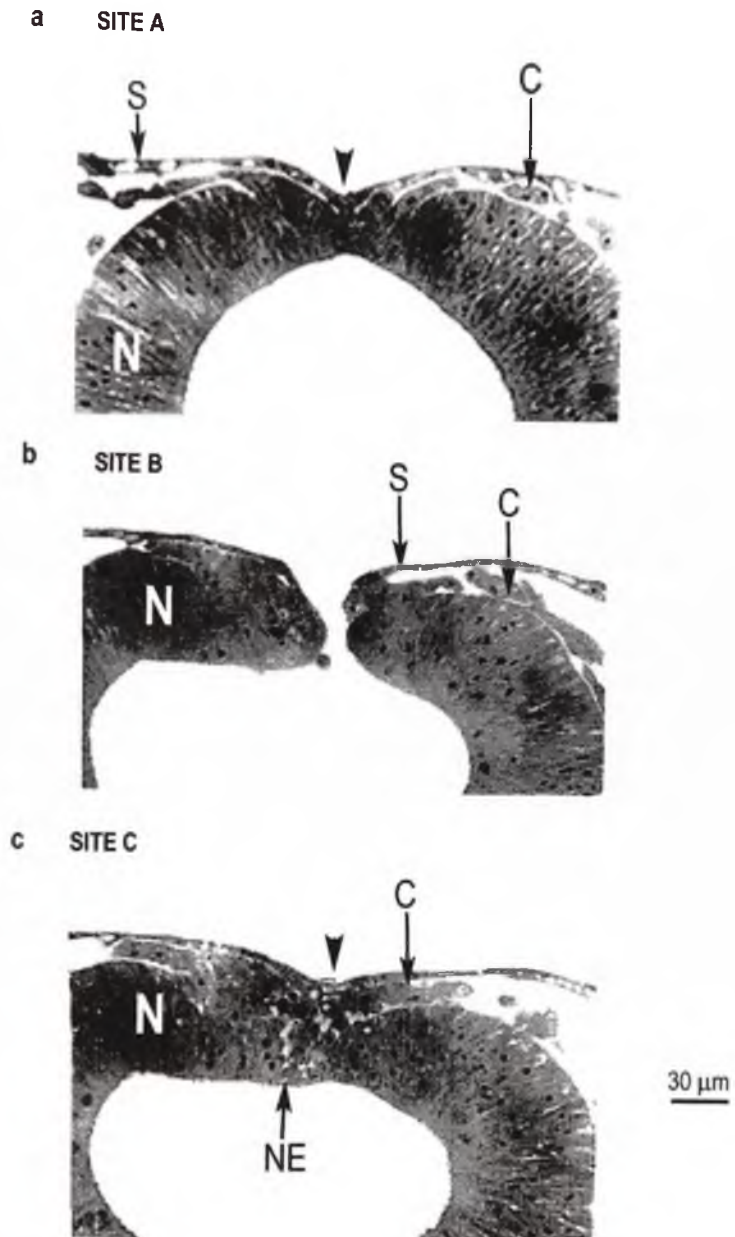


Fig. 8. Transverse LM sections of a r1/r2 wound reincubated for half hour. At sites A and C, the edges of both the surface epithelial (S) and neuroepithelial (N) wounds make contact in the dorsal midline while at site B a gap separates the wound edges. There is a V-shaped depression (*arrowhead*) above the surface epithelium at sites A and C. Note the presence of the neuroepithelial eminence (NE) in c. C-migratory neural crest cells.

3.2.2.2 r1-r3

Wound healing had begun at sites A and C of r1-r3 wounds within 30 minutes of reincubation. Here, the wound edges were in contact with each other. Transverse sections of the wounds showed that the surface epithelial wound edges had fused at sites A and C (Fig. 9a & c). At site B, the surface epithelial wounds still gaped, and the wound edges capped the edges of the neuroepithelial wounds as at zero hour (Fig 9b). Rarely, the gap between the wound edges appeared wider than it was at zero hour. The edges of the neuroepithelial wounds also made contact with each other at sites A and C but were separated by a gap at site B (Fig. 9a, b & c). At site C, the neuroepithelium seemed reduced in its full thickness (cf. Fig. 9c and 8c). Neuroepithelial cells in the immediate vicinity of the neuroepithelial wounds at all three sites were rounded. Additionally, migratory neural crest cells were present between the surface epithelium and neuroepithelium at sites A and B.

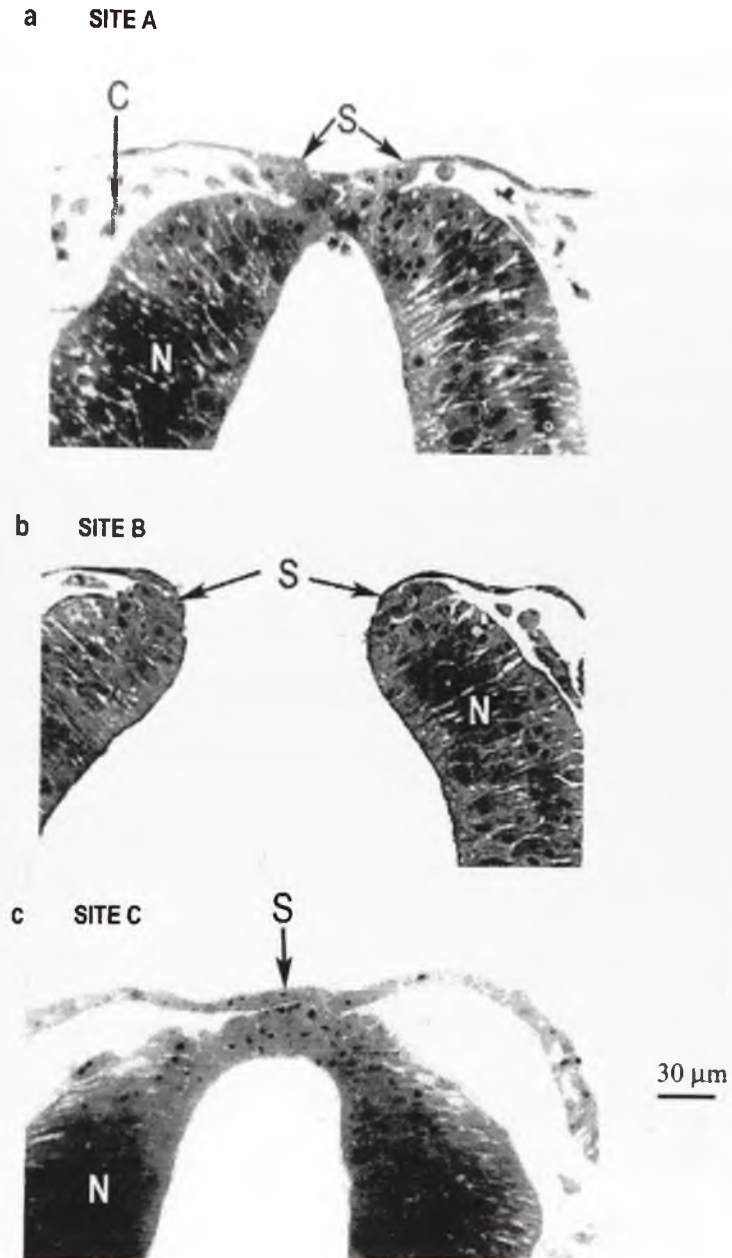


Fig. 9. Transverse LM sections of a r1-r3 wound re-incubated for half hour. At sites A and C, the wound edges of both the surface epithelium (S) and neuroepithelium (N) make contact in the dorsal midline. At site B, a wide gap separates both the surface epithelial and neuroepithelial wounds, with the edges of the surface epithelial layer capping the edges of the neuroepithelial layer. C- migratory neural crest cells.

3.2.3 One-hour reincubation

3.2.3.1 r1/r2

By one hour of re-incubation, the wounds had decreased in length by about 60% (see table 1), and appeared slit-like when examined as whole-mounts. In transverse sections, the appearance of both surface epithelial and neuroepithelial wounds at sites A and C was similar to that at corresponding sites of thirty-minute-old wounds (cf. Figs. 10a & c with 8a & c). At site B, healing had progressed. The edges of both surface epithelial and neuroepithelial wounds were now separated only by a slit-like gap (cf. Fig. 10b with 8b). However, the edges of the surface epithelial wounds still capped the adjacent neuroepithelium (Fig. 10b). The neuroepithelial eminence was present in the caudal part of r1/r2 in only a few embryos. Neuroepithelial cells in the immediate vicinity of the wounds at all three sites were still rounded, and migratory neural crest cells were present between the surface epithelium and neuroepithelium.

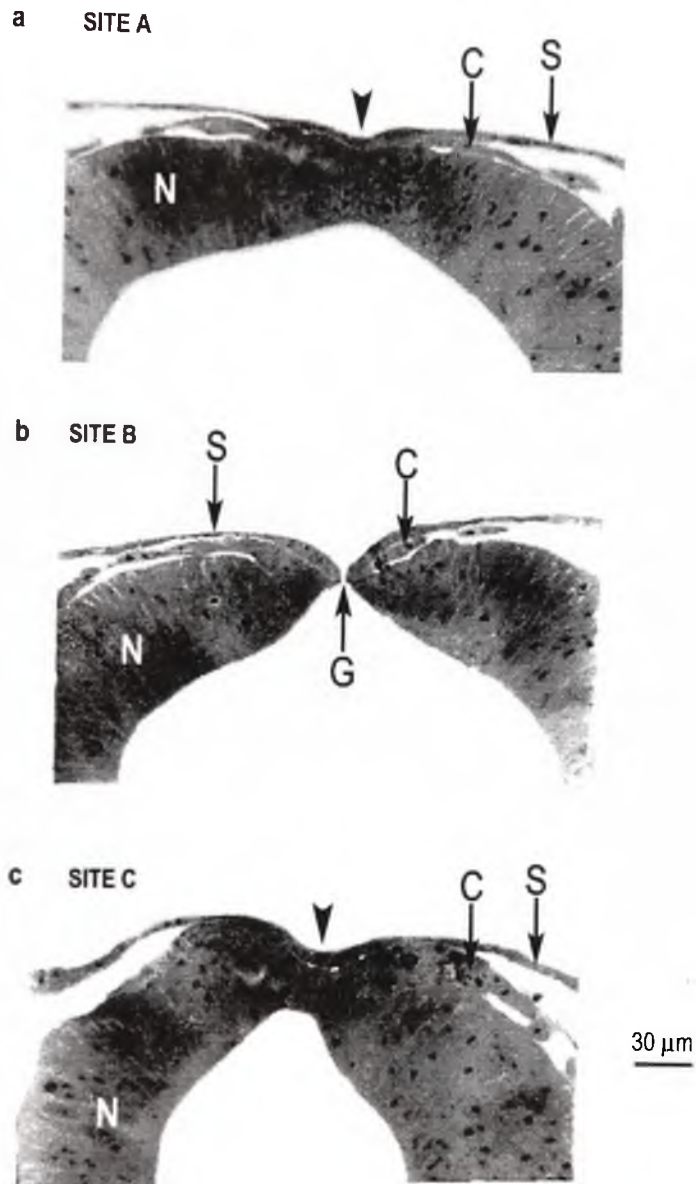


Fig. 10. Transverse LM sections of a r1/r2 wound reincubated for one hour. At sites A and C, the depression over the surface epithelial layer (*Arrowheads*) is still present. At site B, a slit-like gap (*G*) now separates the edges of both the surface epithelial (*S*) and neuroepithelial (*N*) wounds. *C*- migratory neural crest cells.

3.2.3.2 r1-r3

After one hour of re-incubation, there was an average of about 50% decrease in the length of the wounds (see Table 1). Both surface epithelium and neuroepithelium at sites A and C of the r1-r3 wounds did not appear significantly different from those of the half-hour r1-r3 wounds (cf. Fig. 11a with 9a). However, at site B, the gap between the wound edges had significantly reduced (Fig. 11b). Neuroepithelial cells in the immediate vicinity of the wounds at all three sites were rounded after 30 minutes. Migratory neural crest cells were still sandwiched between the surface epithelium and neuroepithelium at sites A and B.

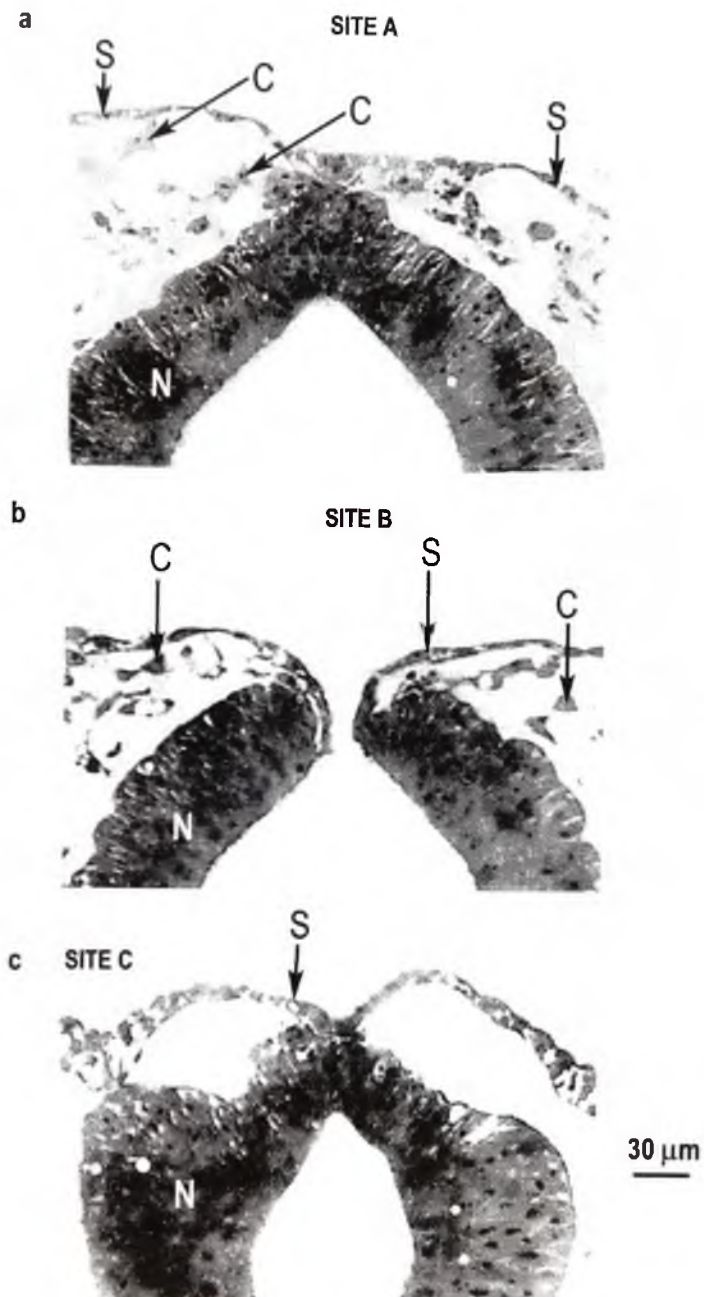


Fig. 11. Transverse LM sections through a r1-r3 wound reincubated for one hour. As in r1/r2 wounds, a slit-like gap separates the the edges of the surface epithelial (S) and neuroepithelial (N) wounds at site B. C- migratory neural crest cells.

3.2.4 Two-hour reincubation

3.2.4.1 r1/r2

After two hours of reincubation, the length of the wounds had decreased by about 95% (see Table 1). At sites A and C there was complete healing of the wounds so that it was difficult to identify these sites. At site B the wounds were represented by a shallow depression. Transverse sections of the wounds showed that at sites A and C the edges of the surface epithelium no longer curled towards the neuroepithelium (Fig. 12a,c). The V” shaped depression that formed above the surface epithelium had therefore disappeared. At site B, the edges of the surface epithelial wounds were now in contact with each other, but they still curled slightly towards the neuroepithelium, creating a shallow V” shaped depression above the fused surface epithelium (cf. Fig 12b with 10b). The appearance of the neuroepithelial wounds at sites A and C was similar to that at sites A and C of one-hour-old r1/r2 wounds. Additionally, the neuroepithelial eminence seen at site C had significantly reduced in size. In some of the embryos, it had disappeared completely. At site B, the edges of the neuroepithelial wounds were now in contact with each other. At all three sites, neuroepithelial cells in the immediate vicinity of the wounds were rounded, and migratory neural crest cells were present between the surface epithelium and the neuroepithelium (Fig. 12a,b,c).

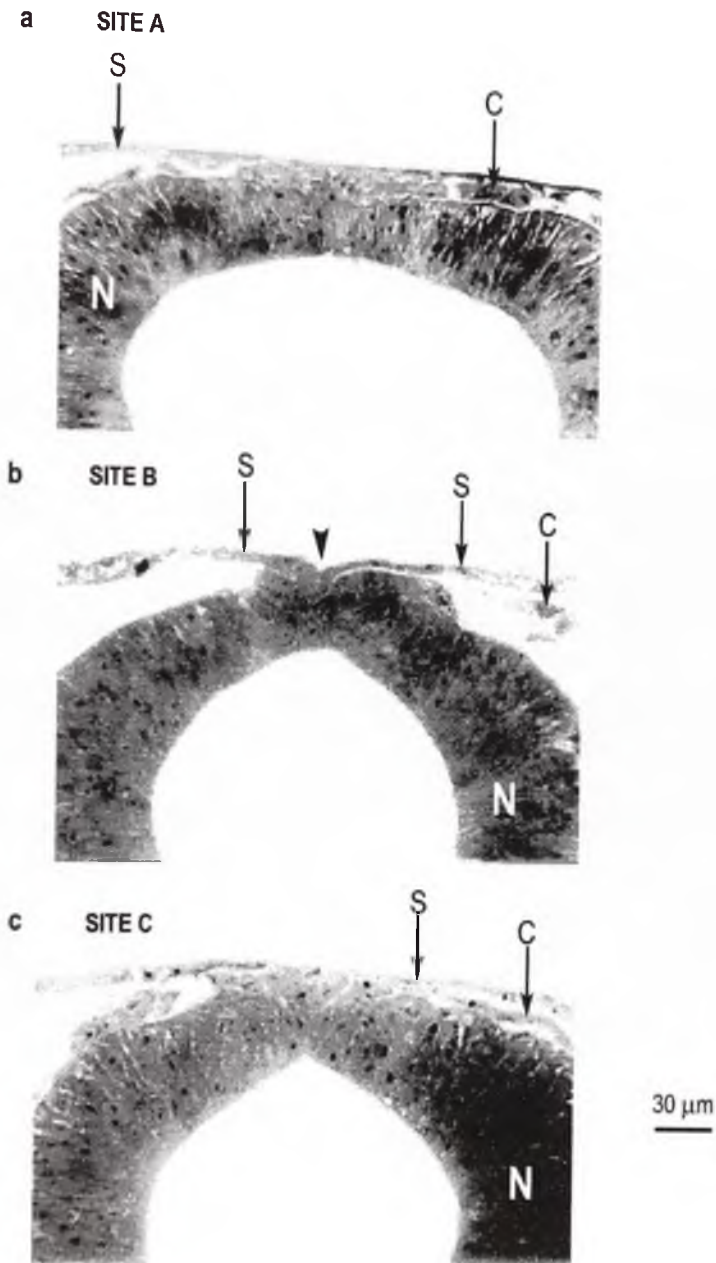


Fig. 12. Transverse LM sections of a r1/r2 wound reincubated for two hours. At site B, the edges of both surface epithelial (*S*) and neuroepithelial wounds (*N*) now make contact in the dorsal midline, with a shallow depression (*Arrowhead*) above the surface epithelial layer. At sites A and C, where complete healing of both surface epithelial and neuroepithelial wounds has occurred, no depression is seen over the surface epithelium. *C*- migratory neural crest cells.

3.2.4.2 r1-r3

After two hours of reincubation, the wounds had decreased in length by about 90% (see Table 1), and appeared slit-like when examined as whole-mounts. Transverse sections of both surface epithelial and neuroepithelial wounds showed that except for the reduction in the full thickness of the neuroepithelium at site C, the wounds at sites A and C appeared similar to those at corresponding sites of one-hour-old r1-r3 wounds (cf. Fig. 13c with 11c). At site B, although a small gap often existed between the edges of both surface epithelial and neuroepithelial wounds, occasionally the edges of the neuroepithelial wound came into contact with each other before that of the surface epithelial wound (See Fig. 13b). In this situation, neuroepithelial wound healing preceded that of surface epithelial wound healing. Neuroepithelial cells in the immediate vicinity of the wounds at all three sites were still rounded, and migratory neural crest cells were sandwiched between the surface epithelium and neuroepithelium at sites A and B.

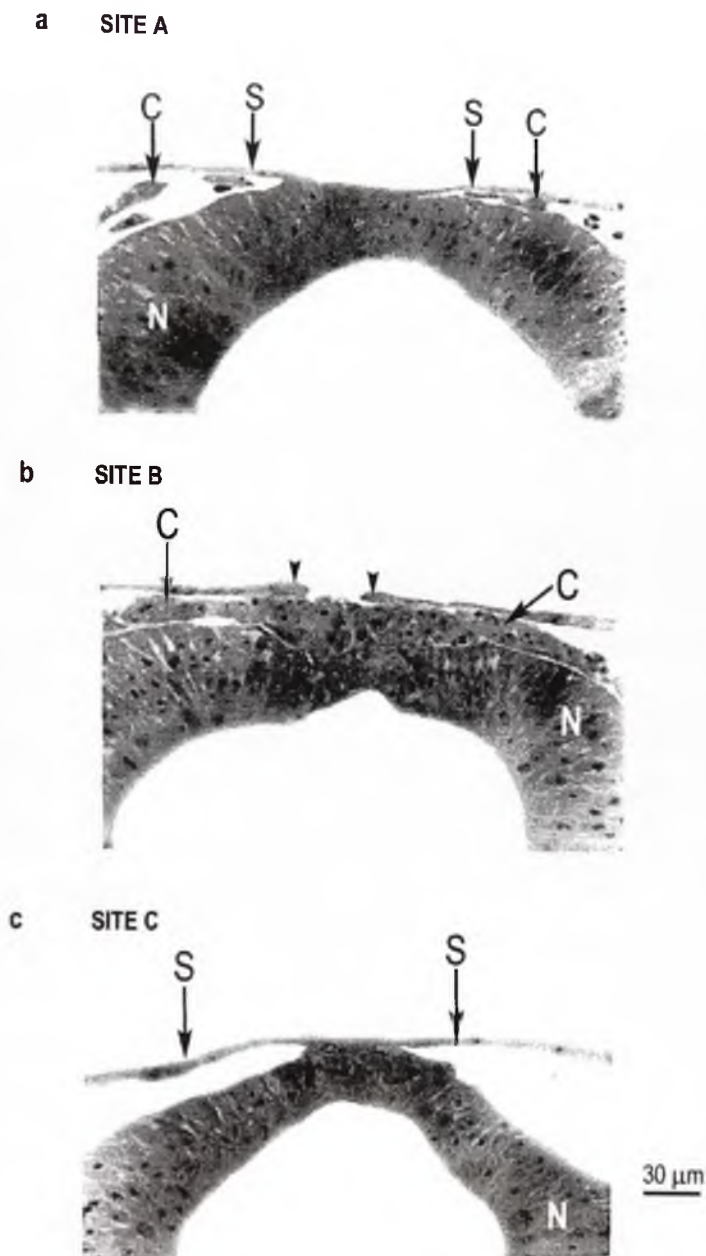


Fig. 13. Transverse LM sections of a r1-r3 wound reincubated for two hours. At site B, the edges of the neuroepithelial wound are in contact with each other, but a slit-like gap separates the edges of the surface epithelial wound (*Arrowheads*). *S*- surface epithelium, *N*- neuroepithelium, *C*- migratory neural crest cells.

3.2.5 Twelve-hour (overnight) reincubation

3.2.5.1 r1/r2 wounds

By twelve hours of reincubation the wounds were healed. Transverse sections of the wounds revealed that there was complete healing of both the surface epithelium and neuroepithelium (Fig. 14a). There was also a significant reduction in the full thickness of the roof plate in the whole extent of each wound (Fig. 14a). The surface epithelium was made up of simple squamous cells, while the neuroepithelium now comprised simple cuboidal cells.

3.2.5.2 r1-r3 wounds

Like the r1/r2 wounds, complete healing of both surface epithelium and neuroepithelium had occurred by twelve hours of reincubation, and the full thickness of the roof plate in r1/r2 and r3 was significantly reduced (Fig. 14b). The surface epithelium and neuroepithelium comprised a single layer of squamous and cuboidal cells respectively. Thinning of the roof plate extended more laterally in r3 (Fig. 14b).

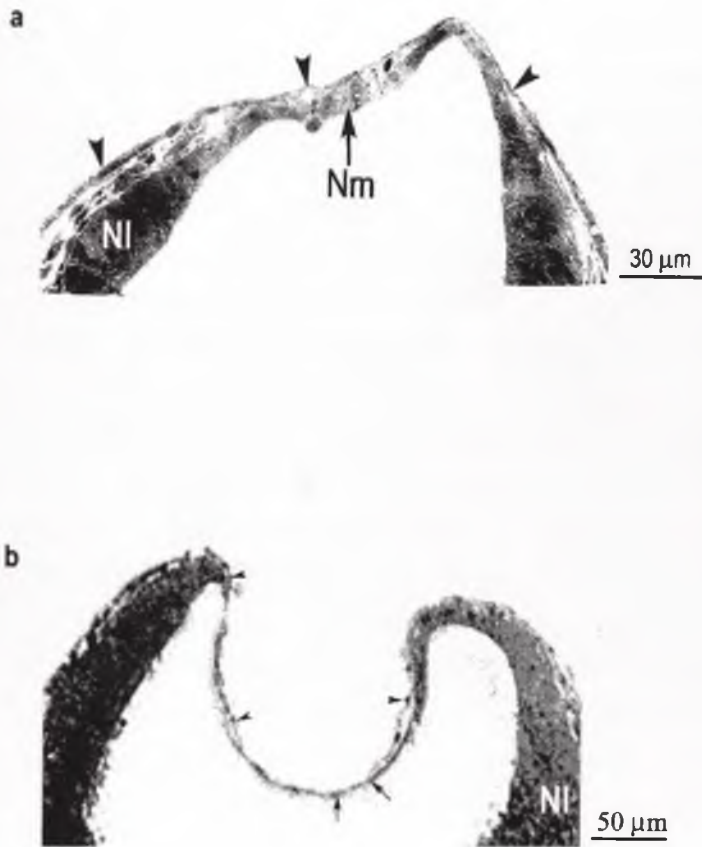


Fig. 14. Transverse LM sections of twelve hour wounds.

(a) a healed wound in r2. The roof plate comprises a single layer of squamous surface epithelial cells (*arrowheads*) and a single layer of cuboidal neuroepithelial cells (*Nm*).

(b) a healed wound in r3. The dorsally placed neuroepithelium (*arrows*) is single layered. Note that thinning of the roof plate is more extensive in b. *NI*- laterally placed neuroepithelium.

Table 1: Comparison between the healing of r1/r2 and r1-r3 wounds.

TIME	LENGTH OF WOUND(μm)		LENGTH CLOSED(μm)		RATE OF HEALING ($\mu\text{m/hr}$)		% OF WOUND HEALED	
	r1/r2	r1-r3	r1/r2	r1-r3	r1/r2	r1-r3	r1/r2	r1-r3
ZERO HOUR	164	232	0	0	0	0	0	0
HALF HOUR	122	176	42	56	84	112	25.6	24.1
ONE HOUR	64	115	100	117	99	117	61	50.4
TWO HOURS	8	24	156	208	78	104	95.1	89.7

Rate of healing

Test of significance using Student's t test ($P < 0.05$) $t = 0.0303$ (significant)

Percentage of wound healed

Test of significance using Student's t test ($P < 0.05$) $t = 0.8434$ (non significant)

Comments

The rate of healing of r1-r3 wounds was significantly faster than that of r1/r2 wounds (Table 1). However, the percentage of the original length of the two wounds (i.e. r1/r2 and r1-r3) closed at any given time did not differ significantly.

3.3 SUMMARY OF WOUND HEALING (FIG. 15)

1. Fresh wounds were slit-like at sites A and C but gaped slightly at site B.
2. The edges of the surface epithelium capped the edges of adjacent neuroepithelium.
3. r1-r3 wounds were longer than r1/r2 wounds.
4. By thirty minutes of reincubation wound healing had begun at the ends (i.e. sites A and C) of the both r1/r2 and r1-r3 wounds, with the edges of both surface epithelial and neuroepithelial wounds making contact with each other in the dorsal midline.
5. After one hour of reincubation, the gap between the wound edges at site B had narrowed.
6. By two hours of reincubation some r1/r2 wounds were already closed.
7. Following twelve hours of reincubation, there was complete healing of both r1/r2 and r1-r3 wounds. Additionally, the roof plate had significantly reduced in its full thickness; it comprised a simple squamous surface epithelium overlying a simple cuboidal neuroepithelium.

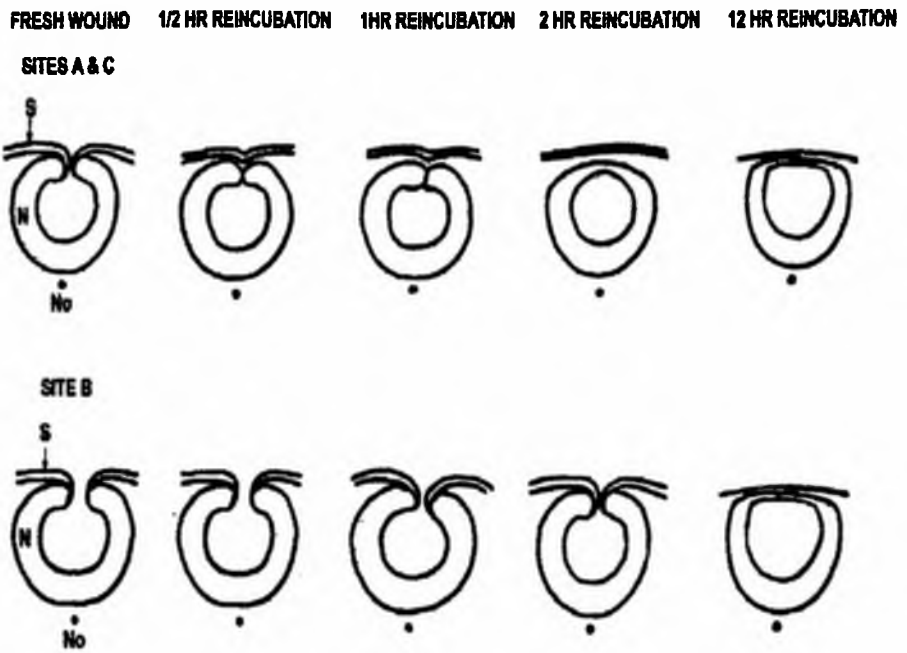


Fig. 15. A line drawing summarising the wound healing process. *No*- notochord, *S*- surface epithelium, *N*- neuroepithelium.

3.4 Acridine orange histochemistry

3.4.1 Control embryos

Examination of control stage 11 and 12 embryos stained with acridine orange showed intense fluorescence in the dorsal midline of r1/r2 and r3 (fig 16a). This showed as punctate fluorescence under the fluorescence microscope. There was a similar intensity of acridine orange staining in r5 and the auditory pits adjacent to this rhombomere (fig 16a).

3.4.2 Wound healing

At zero-hour, fluorescence was observed along the wound edges (Fig. 16b). One hour after the wounds were made, apoptosis was still occurring (Fig. 16c). The distribution of apoptotic cells was similar to what was observed in the fresh wounds. The outline of the wounds, however, now appeared slit-like. By two hours of reincubation, some wounds were already closed (Fig. 16d). In embryos with closed wounds, acridine orange fluorescence was seen in the dorsal midline of r1/r2 as in the controls.

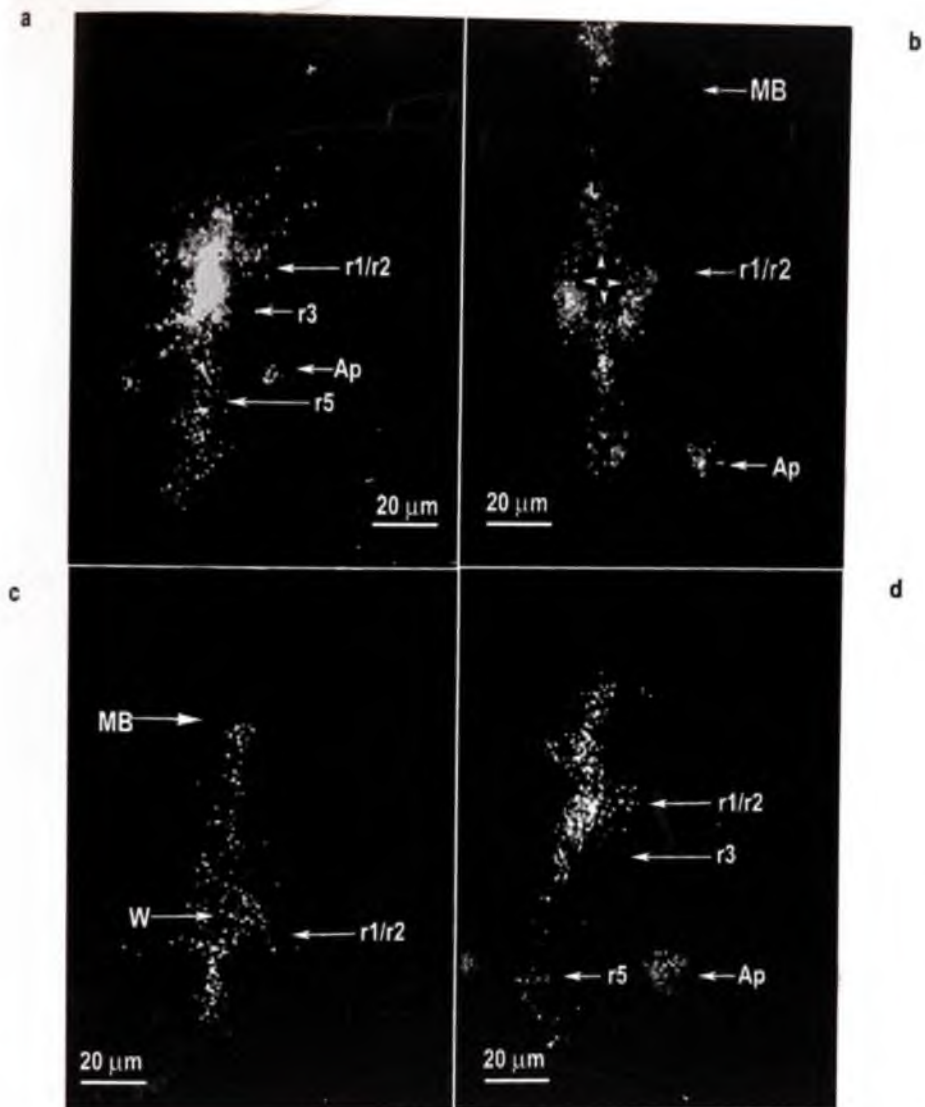


Fig. 16. Acridine orange whole-mount preparations of control and wounded embryos. (a) distribution of apoptosis in a control stage 11 embryo. Apoptosis is intense in r1/r2, r3, r5 and the auditory pits (*Ap*). (b) apoptosis in an embryo with a freshly made r1/r2 wound. Fluorescence is observed along the wound edges (*Arrowheads*) as well. The diamond shaped outline of the wound is due to the flattening of the embryo by the overlying cover slip. (c) apoptosis in an embryo with a one-hour r1/r2 wound. (d) apoptosis in an embryo with a two-hour r1/r2 wound. *W*- wound, *Ap*- auditory pit, *MB*- midbrain, *r*- rhombomeres.

CHAPTER 4

DISCUSSION

4.1 Summary of key findings

Key findings of this study are as follows:

- 1) The hindbrain roof plate at the time it is undergoing apoptosis has the capability to close when it is reopened.
- 2) Wound healing occurs rapidly from the ends of the wound by a zipping-up mechanism in both surface epithelial and neuroepithelial layers. Longer wounds generally heal at a faster rate than shorter ones.
- 3) Apoptosis in the hindbrain roof plate occurs normally in the presence of wound healing, and results ultimately in the thinning of the hindbrain roof plate.

4.2 Response of embryonic tissues to trauma

Several studies on the initial response of embryonic tissues to the trauma of wounding reveal that freshly-made embryonic wounds either gape or appear slit-like (Bellairs *et al.*, 1967; England and Cowper, 1977; Stanisstreet, *et al.*, 1980, 1985; Stanisstreet, 1982; Lawson, 1984; Smedley and Stanisstreet, 1984; Clark and Scothorne, 1990; Lawson and England, 1992, 1996, 1998b; Martin and Lewis, 1992; Brock *et al.*, 1996). It is clear from these studies that the gaping or slit-like appearance of freshly-made wounds may be related to the degree of pre-existing tension in the tissue. The flat blastoderm is under tension, and this causes it to expand underneath the vitelline membrane (New, 1959; Bellairs *et al.*, 1967;

England and Cowper, 1977). Therefore, when any part of it is wounded, tension is released locally at the wound site but continues to act on intact neighbouring cells, causing the wound edges to be pulled apart (England and Cowper, 1977; Stanisstreet, *et al.*, 1980, 1985). This is seen when the endoderm or ectoderm of the early chick blastoderm is wounded (England and Cowper, 1977; Stanisstreet, *et al.*, 1980). Additionally, tension may also build up in a particular embryonic tissue or organ rudiment as it undergoes morphogenesis (Stanisstreet, *et al.*, 1980; Lawson and England, 1992, 1996, 1998b). In chick embryos, for example, the developing brain undergoes a rapid enlargement between stages 16-22 as a result of a rapid accumulation of cerebrospinal fluid (CSF) (Jelinek and Pexieder, 1968, 1970; Desmond and Jacobson, 1977). This results in an increase in tension in the cranial neuroepithelium as well as the surface epithelium overlying it. Thus when the surface epithelial layer overlying the midbrain neuroepithelium is wounded, the wound immediately gapes (Lawson and England, 1996, 1998b). In contrast, at stages 10-12 when the midbrain neuroepithelium and surface epithelium do not seem to be under much tension, wounding the surface epithelium results in the formation of a slit-like rather than a gaping wound (Lawson and England, 1992). In the present study, the response of the hindbrain roof plate to wounding in stages 11 and 12 embryos parallels that of the midbrain surface epithelium and neuroepithelium at similar stages of development. As in the midbrain (see Lawson and England, 1992), tension in the hindbrain at stages 11 and 12 was not high enough to cause the wounds to splay; therefore both hindbrain surface epithelial and neuroepithelial wounds were either slit-like or gaped very slightly at zero hour.

Collectively, the results of the present study and those of previous ones suggest that the level of pre-existing tension in any tissue or developing organ determines the nature of its response to the trauma of wounding, a gaping wound resulting from increased tension and a slit-like wound from low tension.

Another response of embryonic tissues and organ rudiments to the trauma of wounding that may be attributed to the level of pre-existing tension, is the behaviour of the cut edges of the wound. In the present study, the cut edges of the surface epithelial layer curled inwardly (ventrally) to cap the cut edges of the neuroepithelial layer. Thus, the appearance of a freshly-made wound resembles the tips of the neural folds prior to neural fold fusion. This phenomenon whereby the morphology of the edges of the surface epithelial wound cap the neuroepithelium can be attributed to the fact that at these stages (11 and 12), tension in the surface epithelium is not very high. In contrast, at stages 16-22 of development when the level of tension is very high, the edges of a wounded surface epithelial layer are pulled away from the neuroepithelial wound edges, thereby exposing part of the basal surface of the neuroepithelium (Lawson and England, 1998b).

4.3 Characteristics and mechanisms of embryonic wound healing

Previous reports on wound healing indicate that embryonic wounds heal rapidly (England and Cowper, 1977; Stanisstreet, *et al.*, 1980, 1985; Clark and Scothorne, 1990; Lawson and England, 1992, 1996, 1998b; Martin and Lewis, 1992). This may be because the tissues involved are simpler in their organization,

and therefore, may not require the complex processes that are involved in adult wound healing (Martin and Lewis, 1991, 1992; Hopkinson-Woolley *et al.*, 1993; Martin, 1997). In the early chick embryo, for example, healing is complete within about two hours in endodermal and ectodermal wounds (England and Cowper, 1977; Stanisstreet, *et al.*, 1980), and within about five hours in neuroepithelial wounds (Lawson and England, 1992). Even in older chick embryos, complete healing occurs within 24 hours both in the epidermis and neuroepithelium (Martin and Lewis, 1991, 1992; Martin and Nobes 1992; Lawson and England, 1996, 1998b).

In the present study, wound healing was similarly rapid. As early as 30 minutes after wounding, about 25% of the original length of both r1/r2 and r1-r3 wounds was healed. Subsequently, healing of both wounds progressed steadily until final wound closure. That both shorter (r1/r2) and longer (r1-r3) wounds healed in the present study suggests that the size of the wound did not affect its ability to heal. A statistically significant difference was observed between the rates of healing of r1/r2 and r1-r3 wounds, with r1-r3 wounds healing at a faster rate. This might probably be an attempt by the neural tube to seal off the large gap in the r1-r3 wound as fast as possible to prevent neural tube defects from ultimately forming. The observation that at any given time, the average length of wound healed for the two groups (i.e. r1/r2 and r1-r3) did not differ significantly may be a result of the faster rate of healing of r1-r3 wounds.

Another characteristic of embryonic wound healing is the ability of wounds to heal perfectly without the inflammatory response and scar formation that characterise adult wound healing (Whitby and Ferguson, 1991a, 1991b; Martin and Lewis, 1991; McCallion and Ferguson, 1996; Martin 1997). Indeed in the present study, there was no indication of the positions of both surface epithelial and neuroepithelial wounds once complete healing had been effected. This feature of embryonic wounds seems to bear an inverse relationship with the expression of transforming growth factor $\beta 1$ (TGF $\beta 1$), a wound growth factor expressed transiently and at low levels in embryonic wounds, but present at high levels during healing of adult wounds (Whitby and Ferguson, 1991b; Martin *et al.*, 1992; Roberts and Sporn, 1990; Martin, 1997). In mouse embryos, for example, a change in the expression of TGF $\beta 1$ from low to high levels is associated with a transformation from perfect healing without scar tissue formation to healing with scar formation (Hopkinson-Woolley *et al.*, 1993; Martin *et al.*, 1994).

It has been demonstrated that wound healing in the early embryo is effected by cellular behaviours that are similar to those employed in morphogenesis. These include cell migration, cell proliferation, cell rearrangement, changes in cell shape, and tissue fusion (England and Cowper, 1977; Stanisstreet, *et al.* 1980, 1985; Smedley and Stanisstreet, 1984; Schoenwolf, 1985; Schoenwolf and Alvarez, 1989; Schoenwolf and Sheard, 1989; Clark and Scothorne, 1990; Lawson and England, 1992, 1998b; Smith and Schoenwolf, 1997). For example, in the early chick embryo, endodermal wounds heal by the migration of cells at the wound

margins (England and Cowper, 1977), while neuroepithelial wounds heal by tissue fusion (Lawson and England, 1992). On the other hand, ectodermal wounds heal by both changes in cell shape and cell proliferation (Stanisstreet, *et al.*, 1980; Lawson and England, 1998b). Additionally, the contraction of actin filaments in the form of a purse-string is employed in the healing of epidermal wounds in older embryos (Martin and Lewis, 1992; Brock *et al.*, 1996).

The results of previous studies indicate that the mechanism of wound healing in a particular embryonic tissue may be dependent on a number of factors, including the structure and organisation of the tissue (England and Cowper, 1977; Stanisstreet, *et al.*, 1980), and the level of tension in the tissue during wound healing (Lawson and England 1996, 1998b). The difference in the healing mechanisms of the early endoderm and ectoderm, for instance, is attributable to the differences in the structure and organisation of these tissues. The chick endoderm rests on a substrate formed by the epithelial basal lamina, which is present even in the unincubated egg (Low, 1967; Sanders, 1979). Additionally, junctional complexes between the endodermal cells are poorly developed at this stage of development. Therefore, the cells at the wound edges freely dissociate from each other and migrate using the epithelial basal lamina as a substrate to effect wound healing (England and Cowper, 1977). In contrast, when the ectoderm is wounded, neither the endoderm nor the head mesenchyme underlying it provides a coherent basal lamina that can be used as a substrate for the migration of marginal cells to effect healing. Moreover, ectodermal cells at the wound edges do not freely

dissociate from each other as their junctional complexes are highly developed (Trelstad *et al.*, 1967). Wound healing in the early embryonic ectoderm, therefore, occurs mainly through a change in cell shape, aided by cell proliferation (Stanisstreet, *et al.* 1980; Lawson and England 1996, 1998b). In older embryos, the ectoderm gives rise to the epidermis, which has a more complex structure. It is a stratified layer with a cuboidal basal layer overlain by a squamous peridermal layer. Here, wounds are known to heal principally by a contraction of an actin cable assembled at the wound margins of the basal epidermal layer a few minutes after wounding (Martin and Lewis, 1992; Brock *et al.*, 1996). According to these authors, contraction of this cable of actin filaments, like a purse-string, serves to draw the wound margins together to effect healing.

The second factor that influences embryonic wound healing is the level of tension in the tissue (Clark and Scothorne, 1990; Lawson and England, 1996, 1998b). When tension is low, complete healing occurs since the wound edges remain slit-like or gape very slightly, permitting physical contact between the wound edges (Lawson and England, 1992; Clark and Scothorne, 1990). In contrast, when the tension in the tissue is high, the edges of a wound splay, preventing the required physical contact between the wound edges to effect healing (Lawson and England, 1996, 1998b). In a classical experiment to demonstrate the importance of tension in embryonic wound healing, Lawson and England (1996) reduced tension at the edges of non-healing midbrain neuroepithelial wounds, and observed that rapid healing of the midbrain neuroepithelium occurred. In a similar study, they reduced

tension at the two ends of both non-healing and healing surface epithelial wounds in chick embryos at stages 16-20 (Lawson and England, 1998b). Here, there was a rapid and complete healing of the wounds that previously did not heal, and about 162.5% increase in the rate of healing of wounds that normally healed. Collectively, these results prove that tension is an important factor in embryonic wound healing.

In the present study, closure of both surface epithelial and neuroepithelial wounds started from the ends of the wounds and proceeded in a zipper-like manner towards the middle portion of the wound. This pattern of wound healing observed in these tissues may be related to the level of tension existing in them at the stages used, for at stages 11 and 12, tension in these tissues was not high enough to cause the edges of the linear wounds to be pulled far apart. Thus, the wound edges gaped very slightly in the middle portion of the wound, while they were separated only by a slit-like gap at the ends of the wound. Therefore, wound healing began at the two ends of the wounds where physical contact between the wound edges was easily established at the start of the healing process, and then progressed in a zipper-like manner towards the middle portion of the wound.

In the present study, healing of the surface epithelial wound occurred first, followed by healing of the neuroepithelial wound. A reason for this may be that the edges of the surface epithelium capped the edges of the neuroepithelium, making it impossible for apposition of the neuroepithelial wound edges to occur first.

However, following the healing and delamination of the surface epithelium from the neuroepithelium, apposition and healing of the neuroepithelial wound edges ensued. The nature of the cells that effected the healing of the hindbrain neuroepithelial wound is of interest. It has been suggested that at the early stages of development, progenitor neural crest cells have the ability to form neuroepithelial cells (Bronner-Fraser, 1995; Bronner-Fraser and Fraser, 1989). One may thus be tempted to conclude that at the time that neuroepithelium in the dorsal midline of the hindbrain undergoes massive apoptosis, it is possible that progenitor neural crest cells would contribute the cells needed to effect wound healing in the hindbrain. However, there is evidence to suggest the involvement of a sub population of hindbrain neuroepithelial cells (Lawson and England, 1998a; Lawson *et al.*, 1999). Lawson *et al.* (1999) have demonstrated the presence of a subpopulation of neuroepithelial cells in the hindbrain roof plate that do not undergo apoptosis. According to them, these cells rearrange themselves to reform the neuroepithelial layer of the hindbrain roof plate after apoptosis has ceased (Lawson and England, 1998a). It is therefore likely that some or all of these neuroepithelial cells might have participated in the healing of the neuroepithelial wound in the present study.

4.4 Wound healing and morphogenesis

Previous studies on embryonic wound healing have shown that the healing capability of a wounded tissue or an organ rudiment may be affected by the nature of morphogenetic processes occurring during wound healing (Clark and Scothorne,

1990; Lawson and England, 1996; 1998b). For example, whereas midbrain neuroepithelial wounds heal completely during the formation of the neural tube (Lawson and England, 1992), there is a marked reduction in the healing capability of the midbrain neuroepithelium at a time when rapid morphogenetic brain expansion occurs (Lawson and England, 1996). Lawson *et al.*, (1999), on the basis of their findings that massive apoptosis occurs in the hindbrain roof plate, hypothesized that apoptosis may render the hindbrain roof plate incapable of healing when damaged, leading to the formation of neural tube defects.

The present study, which was partly aimed at testing this hypothesis has, however, clearly demonstrated that wound healing in the hindbrain neuroepithelium is not directly affected by the major morphogenetic processes occurring in this portion of the neuraxis, namely, apoptosis and thinning of the hindbrain roof plate. Indeed, the wounds ultimately healed completely despite the high levels of apoptosis in the hindbrain. It is therefore not likely that apoptosis had a detrimental effect on the healing process. Therefore, if neural tube defects should develop in the hindbrain through a reopening of its roof plate, the process is likely to be due to factors other than apoptosis. Taken together, the above results demonstrate that the nature of morphogenetic processes occurring in any part of the neuraxis plays a key role in determining whether an assault to that part will result in neural tube defects or not. Morphogenetic processes that prevent the edges of a wound from coming together ultimately prevent wound healing from taking place, thereby leading to the formation of neural tube defects. On the other hand, if the morphogenetic

processes permit the apposition of the wound edges, wound healing occurs, and neural tube defects are not formed.

There is also evidence to suggest that neural tube wound healing affects normal neural tube morphogenesis in embryos (Clark and Scothorne, 1990; Lawson and England, 1996). Lawson and England (1996), in their studies on wound healing in the midbrain of the chick embryo at stages 18-22, demonstrated the effects of neural tube wound healing on morphogenetic brain expansion. Here, healing failed to occur, exposing the apical surfaces of the neuroepithelial cells to the external environment. Additionally, the cavity of the midbrain was significantly reduced to an irregular slit by the intense folding of the walls of the neuroepithelium. As a result of this, morphogenetic brain expansion failed to occur and neural tube defects resulted. Clark and Scothorne (1990) in a similar study, demonstrated that in embryos at stages 17 and 18, the inability of wounds to heal in the spinal cord region of the neural tube has deleterious effects on the occlusion of the neural canal in this part of the neuraxis. The latter morphogenetic process, namely, spinal canal occlusion, is required for normal expansion of the cranial portion of the neuraxis (Schoenwolf and Desmond, 1984). In the hindbrain region, however, the present study has shown that wound healing does not appear to influence the main morphogenetic process occurring in this portion of the neuraxis, namely, thinning of the roof plate. Indeed, acridine orange histochemistry showed that apoptosis occurred normally in spite of wound healing, resulting in the thinning of the hindbrain roof plate. It is clear from the results of the present study that apoptosis

in the hindbrain roof plate is neither arrested nor reversed during wound healing. It is interesting that the early embryo has in place reparative mechanisms that ensure that assaults to it are taken care of, thereby preventing the interference of normal morphogenetic processes.

The present study also demonstrates similarities in the processes of neural tube wound healing and neural fold fusion in the hindbrain of the chick embryo. In the zero hour wound, the cut edges of the surface epithelial layer cap the cut edges of the neuroepithelial layer in much the same way that the surface epithelial layers of the bilateral neural folds cap the neuroepithelial layers prior to neural fold fusion (Lawson and England, 1998a). Like hindbrain neural fold fusion therefore, healing of the surface epithelial layer occurs first, followed by healing of the neuroepithelial layer once the former has delaminated from it. It has been suggested that the migration of cephalic neural crest cells may contribute to surface epithelial fusion during neurulation (Lawson and England 1998a). According to Lawson and England (1998a), the neural crest cells may help push the edges of the surface epithelial layers of the neural folds medially as they migrate to enhance fusion. In the present study, the presence of neural crest cells immediately deep to the healing surface epithelial layer may in a similar fashion enhance surface epithelial wound healing at these stages.

REFERENCES

- Alvarez, I.S. and Schoenwolf, G.C. (1992). Expansion of surface epithelium provides the major extrinsic force for bending of the neural plate. *Journal of Experimental Zoology* **261**:340-348.
- Anderson, C.B. and Meier, S. (1981). The influence of the metameric pattern in the mesoderm on migration of neural crest cells in the chick embryo. *Developmental Biology* **85**:385-402.
- Bancroft, M. and Bellairs, R. (1975). Differentiation of the neural plate neural folds in the young chick embryo. *Anatomy and Embryology* **147**:309-335.
- Bellairs, R., Bromham, D.R. and Wylie, C.C. (1967). The influence of the area opaca on the development of the young chick embryo. *Journal of Embryology and Experimental Morphology* **17**:195-212.
- Brock, J., Midwinter, K., Lewis, J. and Martin, P. (1996). Healing of incisional wounds in the embryonic chick wing bud: characterisation of the actin pulse-string and demonstration of a requirement for Rho activation. *Journal of Cell biology* **135**:1097-1107.
- Bronner-Fraser, M. (1995). Origins and development potential of the neural crest. *Experimental Cell Research* **218(2)**:405-417.
- Bronner-Fraser, M. and Fraser, S. (1989). Development potential of avian trunk neural in situ. *Neuron* **3(6)**:755-766.

- Clark, B.J. and Scothorne, R.J. (1990). Variation in the response of chick embryo to incision of the roof plate of the neural tube at different developmental stages. *Journal of Anatomy* **168**:167-184.
- Colas, J-F. and Schoenwolf, G.C. (2001). Towards a cellular and molecular understanding of neurulation. *Developmental Dynamics* **22**:117-145.
- Copp, A.J., Brook, F.A., Estibeiro, J.P., Shum, A.S.W. and Cockroft, D.L. (1990). The Embryonic development of mammalian neural tube defects. *Progress In Neurobiology* **35**:363-403.
- Copp, A.J., Brook, F.A. (1989). Does lumbosacral spina bifida arise by failure of neural folding or by defective canalisation. *Journal of Medical Genetics* **26(3)**: 160-166.
- Desmond, M.E. and Jacobson, A.G. (1977). Embryonic brain enlargement requires cerebrospinal fluid pressure. *Developmental Biology* **57**:188-198.
- England, M.A. and Cowper, S.V. (1977). Wound healing in the early chick embryo studied by scanning electron microscopy. *Anatomy and Embryology* **152**:1-4.
- Freeman, B.G. (1972). Surface modifications of neural epithelial cells during formation of the neural tube in the rat. *Journal of Embryology and Experimental Morphology* **28**:437-448.
- Geelen, J.A.G. and Langman, J. (1977). Closure of the neural tube in cephalic region of the mouse embryo. *The Anatomical Record* **189**:625-640.
- Geelen, J.A.G. and Langman, J. (1979). Ultrastructural observayion on closure of the neural tube in the mouse. *Anatomy and Embryology* **156**:73-88.

- Gerschenson, L.E. and Rotello, R.J. (1992). Apoptosis: a different type of cell death. *FASEB Journal* **6**:2450-2455.
- Gillette, R. (1944). Cell number and cell size in the ectoderm during neurulation (*Amblystoma maculatum*). *Journal of Experimental Zoology* **96**:201-222.
- Glaser, O. (1914). On the mechanism of morphological differentiation in the nervous system- the transformation of a neural plate into a neural tube. *The Anatomical Record* **8**:525-551.
- Glucksmann, A. (1951). Cell death in normal vertebrate ontogeny. *Biological Review* **26**:59-86.
- Hackett, D.A., Smith, J.L. and Schoenwolf, G.C. (1997). Epidermal ectoderm is required for full elevation and for convergence during bending of the avian neural plate. *Developmental Dynamics* **210**:397-406.
- Hamburger, V and Hamilton, H.L. (1951). A series of normal stages in the development of the chick embryo. *Journal of Morphology* **88**:49-92.
- Handel, M.A. and Roth, L.E. (1971). Cell shape and morphology of the neural tube: Implications for microtubule function. *Developmental Biology* **25**:78-95.
- His, W. (1874). Unsere Korperform, und das Physiologische Problem Ihrer Entstehung. F.C.W. Vogel, Leipzig.
- Hopkinson-Wooley, J., McCluskey, J., Lewis, J. and Martin, P., (1993). Clinical implications of embryonic wound healing. *Journal of Wound Care* **2**:158-161.

- Ishii, K. (1967). Morphogenesis of the brain in medaka, *oryzias latipes* I. Observations on Morphogenesis. *Scientific Report of Tohoku University Series IV (Biology)* **33**:97-104.
- Jacobson, A.G. (1981). Morphogenesis of the neural plate and tube. In: *Morphogenesis and Pattern formation*. (T.G. Connelly, L.L. Brinkley, B.N. Carlson, Eds.) Raven Press, New York. pp 233-260.
- Jacobson, A.G. and Tam, P.P.L. (1982). Cephalic neurulation in the mouse embryo analyzed by SEM and morphometry. *The Anatomical Record* **203**:375-396.
- Jaskoll, T., Greenbeg, G. and Melnick, M. (1991). Neural tube and neural crest: A new view with time-lapse high-defination photomicroscopy. *American Journal of Medical Genetics* **41**:333-345.
- Jelinek, R. and PeXeieder, T. (1968). The pressure of encephalic fluid in chick embryos between the 2nd and 6th day of incubation. *Physiologia Bohemoslov* **17**:297-305.
- Jelinek, R. and PeXeieder, T. (1970). Pressure of CSF and the morphogenesis of CNS in chick embryo. *Folia Morphologia (Warsz)* **18**:102-110.
- Karfunkel, P. (1971). The role of microtubules and microfilaments in neurulation in *Xenopus*. *Developmental Biology* **25**:30-56.
- Karfunkel, P. (1972). The activity of microtubules and microfilaments in neurulation in the chick. *Journal of Experimental Zoology* **38**:289-302.
- Karfunkel, P. (1974). Mechanism of neural tube formation. *International Review Of Cytology* **38**:245-271.

- Lawson, A. (1984). Studies on neural tube wound healing in the chick embryo. PhD Thesis. Department of Anatomy, University of Leicester. pp 1-99, 234
- Lawson, A and England, M.A. (1992). Studies on wound healing in the neuroepithelium of the chick embryo. *The Anatomical Record* **233**:291-300.
- Lawson, A and England, M.A. (1996). Effect of embryonic cerebrospinal fluid pressure and morphogenetic brain expansion on wound healing in the midbrain of the chick embryo. *Anatomy and Embryology* **193**:601-610.
- Lawson, A and England, M.A. (1997). Neural tube Defects: How do they arise in the chick embryo. *West Africa Journal of Anatomy* **5**:1-8.
- Lawson, A and England, M.A. (1998a). Neural fold fusion in the cranial region of the chick embryo. *Developmental Dynamics* **212**:473-481
- Lawson, A and England, M.A. (1998b). Surface ectodermal wound healing in the chick embryo. *Journal of Anatomy* **192**:497-506.
- Lawson, A., Schoenwolf, G.C., England, M.A., Addai, F.K. and Ahima, R.S. (1999). Programmed cell death and the morphogenesis of the hindbrain roof plate in the chick embryo. *Anatomy and Embryology* **200**:509-519.
- Lawson, A., Anderson, H. and Schoenwolf, G.C. (2001). Cellular mechanisms of neural fold formation and morphogenesis in the chick embryo. *The Anatomical Record* **262**: 153-168.
- Lee, H-Y, Sheffield, J.B. and Nagele, R.G. (1978). The role of extracellular matrix in chick neurulation II. Surface morphology of neuroepithelial cells during neural fold fusion. *Journal of Experimental Zoology* **204**:137-154.

- Low, F.N (1967). Developing boundary (basement) membranes in the chick embryo. *The Anatomical Record* **159**:231-238.
- Lumsden, A., Sprawson, N. and Graham, A. (1991). Segmental origin and migration of neural crest cells in the hindbrain region of the chick embryo. *Development* **113**:1281-1291
- Mak, L.T. (1978). Ultrastructural studies of amphibian neural fold fusion. *Developmental Biology* **65**:435-446.
- Martin, A.H. (1967). Significance of mitotic spindle fibre orientation in the neural tube. *Nature* **216**:1133-1134.
- Martin, P. (1997). Wound healing – aiming for perfect skin regeneration. *Science* **276**:75-81.
- Martin, P. and Lewis, J. (1991). The mechanisms of embryonic wound healing: limb-bud lesions in mouse and chick embryos. In: *Foetal Wound healing*. (Adzick, N.S. and Longaker, M.T., Eds.) Elsevier, New York.
- Martin, P. and Lewis, J. (1992). Actin cables and epidermal movements in Embryonic wound healing. *Nature* **360**:179-182.
- Martin, P. and Nobes, C.D. (1992). An early molecular component of the wound healing Response in rat embryos- induction of c-fos protein in cells at the epidermal wound margin. *Mechanisms of Development* **38**:209-216.
- Martin, P., Hopkinson-Wooley, J. and McCluskey, J. (1992). Growth factors and cutaneous wound repair. *Progress in Growth Factor Research* **4**:25-44.
- Martin, P. Nobes, C.D., McCluskey, J. and Lewis J. (1994). Repair of excisional wounds in the embryo. *Eye* **8**:155-160.

- Martin-Partido, G., Alvarez, S., Rodriguez-Gallardo, L and Narascues, J. (1985). Differential staining of dead and dying embryonic cells with a simple new technique. *Journal of Microscopy* **12**:101-106.
- McCallion R.L. and Ferguson, M.W.J. (1996). Foetal wound healing and the development of anti-scarring therapies for adult wound healing. In *The Molecular and Cellular Biology of Wound Healing* (ed. Clark, R.A.F) pp. 561-600. New York: Plenum.
- Messier, P.E. (1969). Effects of β -mercaptoethanol on the fine structure of the neural plate cells of the chick embryo. *Journal of Embryology and Experimental Morphology* **21**:309-329.
- Moran, D. and Rice, R.W. (1975). An ultrastructural examination of the role of cell membrane surface coats material during neurulation. *Journal of Cell Biology* **64**:172-181.
- Morgagni, J.B. (1769). The seats and causes of disease investigated by Anatomy (*English Translation: Benjamin Alexander*) London: Miller and Cadel.
- Morriss, G.M. and New, D.A.T. (1979). Effect of oxygen concentration on morphogenesis of cranial neural folds and neural crest in cultured rat embryos. *Journal of Embryology and Experimental Morphology* **46**:37-52.
- Morriss-Kay, G., Wood, H. and Chen, W-H. (1994). Normal neurulation in mammals. *Ciba foundation symposium* **181**:51-69. Chichester, U.K:Wiley.

- Moury, J.D. and Schoenwolf, G.C. (1995). Cooperative model of epithelial shaping and bending during avian neurulation: Autonomous movements of the neural plate, autonomous movements of the epidermis, and interactions in the neural plate/epidermis transition zone. *Developmental Dynamics* **204**:323-337.
- Myrianthopoulos, N. C. and Melnick, M. (1987). Studies in neural tube defects I. epidemiologic and aetiologic aspects. *American Journal of Medical Genetics* **26**:783-796.
- New, D.A.T. (1955). A new technique for the cultivation of the chick embryo *in vitro*. *Journal of Embryology and Experimental Morphology* **3**:326-331.
- New, D.A.T. (1959). The adhesive properties and expansion of the chick blastoderm. *Journal of Embryology and Experimental Morphology* **7**:146-164.
- O’Rahilly, R. and Gardner, E. (1979). The initial development of the human brain. *Acta Anatomica* **104**:123-133.
- Portch, P.A. and Barson, A.J. (1974). Scanning electron microscopy of neurulation in the chick. *Journal of Anatomy*. **117**:341-350.
- Poznanski, A., Minsuk, S., Stathipoulos, D. and Keller, R. (1997). Epithelial cell wedging and neural trough formation are induced planarly in *Xenopus*, without persistent vertical interactions with mesoderm. *Developmental Biology* **189**:26-269.

- Rice, R.W. and Moran, D.J. (1977). A scanning electron microscopic and x-ray microanalytic study of cell surface material during neurulation. *Journal of Experimental Zoology* **201**:471-478.
- Roberts, A.B. and Sporn, M.B. (1990). The transforming growth factors s. In *Peptides growth factors and their receptors* (M.B. Sporn & A.B. Roberts, eds), pp 419-472.
- Roux, W. (1885). Beitrage zur entwicklungsmechanik des embryo. *Zell Biologie* **21**:411-526.
- Rugh, R. (1951). The frog: its reproduction and development. McGraw-Hill, New York, pp 123-138.
- Sadler. T.W. (1978). Distribution of surface coat material on fusing neural folds of the mouse embryos during neurulation. *The Anatomical Record* **191**:345-350.
- Sadler. T.W. (2000). Molecular regulation of neural induction. *Langman's Medical Embryology 8th edition*. Lippincot William and Wilkins, Philadelphia. p 83.
- Sakai, (1989). Neurulation in the mouse: manner and timing of neural tube closure. *The Anatomical Record* **223**:194-203.
- Sakai, Y. and Yamamura, H. (1979). Mechanism of the neural tube formation IV. Regional sequence and somite stage of fusion of the cranial neural folds in mouse embryos. *Kaibogaku Zasshi* **54**:97-98. (Abstract)
- Sanders, E.J. (1979). Development of the basal lamina and extracellular matrix in The early chick embryo. *Cell Tissue Research* **198**:527-537.

- Sausedo, R.A., Smith, J.L. and Schoenwolf, G.C. (1997). Role of non-randomly oriented cell division in shaping and bending of the neural plate. *Journal of Comparative Neurology* **381**:473-488.
- Schmitz, B., Papan, C. and Campos-Ortega, J.A. (1993). Neurulation in the anterior trunk of the zebra fish (*Brachydanio rerio*). *Developmental Biology* **202**:250-259.
- Schoenwolf, G.C. (1978). An SEM study of posterior spinal cord development in the chick embryo. *Scanning Electron Microscopy/1978/II*: 739-746.
- Schoenwolf, G.C. (1982). On the Morphogenesis of the early rudiments of the developing central nervous system. *Scanning Electron Microscopy/1982/1*:289-308.
- Schoenwolf, G.C. (1983). The chick epiblast: a model for examining epithelial morphogenesis. *Scanning Electron Microscopy/1983/III*: 1371-1385.
- Schoenwolf, G.C. (1984). Histological and Ultrastructural studies of secondary neurulation in mouse embryos. *American Journal of Anatomy* **169**:361-376.
- Schoenwolf, G.C. (1985). Shaping and bending of the avian neuroepithelium: Morphometric analysis. *Developmental Biology* **109**: 127-139.
- Schoenwolf, G.C. (1988). Microsurgical analysis of avian neurulation: Separation of medial and lateral tissues. *Journal of Comparative Neurology* **276**:498-507

- Schoenwolf, G.C. (1994). Formation and patterning of the avian neuraxis; one dozen hypotheses. In: Neural tube defects *Ciba foundation symposium* **181**:25-50. Chichester, U.K:Wiley.
- Schoenwolf, G.C. and Alvarez, I.S. (1989). Roles of neuroepithelial cell rearrangement and cell division in shaping of the avian neural plate. *Development* **106**:427-439.
- Schoenwolf, G.C. and Alvarez, I.S. (1991). Specification of neuroepithelium and surface epithelium in avian transplantation chimeras. *Development* **112**:713-722.
- Schoenwolf, G.C. and Delongo, (1980). Ultrstructure of secondary neurulation in the chick embryo. *American Journal of Anatomy* **158**:43-63.
- Schoenwolf, G.C. and Desmond, M.E. (1984). Descriptive studies of occlusion and reopening of the spinal cord of the chick embryo. *The Anatomical Record* **209**:251-263.
- Schoenwolf, G.C. and Franks, M.V. (1984). Quantitative analyses of changes in cell shapes during bending of the neural plate. *Developmental Biology* **105**:257-272.
- Schoenwolf, G.C. Powers, M.L. (1987). Shaping of the chick neuroepithelium during primary and secondary neurulation: Role of cell elongation. *The Anatomical Record* **218**:182-195.
- Schoenwolf, G.C. Sheard, P. (1989). Shaping and bending of the avian neural plate as analyzed with the fluorescent-histochemical marker. *Developmental Biology* **105**:17-25.

- Schoenwolf, G.C. and Smith, J.L. (1990a). Mechanisms of neurulation: traditional viewpoint and recent advances. *Development* **109**:342-270.
- Schoenwolf, G.C. and Smith, J.L. (1990b). Epithelial cell wedging: a fundamental cell behaviour contributing to hinge point formation during epithelial morphogenesis. *Seminars in Developmental Biology* **1**:325-334.
- Shroeder, T.E. (1970). Neurulation in *Xenopus laevis*. An analysis and model based on light and electron microscopy. *Journal of Embryology and Experimental Morphology*. **23**:427-462.
- Silver, M.N. and Kerns, J.M. (1978). Ultrastructure of neural fold fusion in chick embryos. *Scanning Electron Microscopy Vol. II*:209-216.
- Smedley, M.J. and Stanisstreet, M. (1984). Scanning electron microscopy of wound healing in rat embryo. *Journal of Embryology and Experimental Morphology* **83**:109-117.
- Smith, J.L. and Schoenwolf, G.C. (1987). Cell cycle and neuroepithelial cell shape during bending of the chick neural plate. *The Anatomical Record* **218**:196-206.
- Smith, J.L. and Schoenwolf, G.C. (1988). Role of cell cycle in regulating neuroepithelial cell shapes during bending of the chick neural plate. *Cell Tissue Research* **252**:491-500.
- Smith, J.L. and Schoenwolf, G.C. (1997). Neurulation: coming to closure. *Trends in Neuroscience* **20** 510-517.

- Smith, J.L., Schoenwolf, G.C. and Quan, J. (1994). Qualitative analysis of neuroepithelial cells shapes during bending of mouse neural plate. *Journal of Comparative Neurology* **342**:144-151.
- Stanisstreet, M. (1982). Calcium and wound healing in *Xenopus* early embryos. *Journal of Embryology and Experimental Morphology* **67**:195-205.
- Stanisstreet, M., Smedley, M.J. and Snow, R.M. (1985). Tension and wound healing in amphibian early embryos. *Acta Embryologia Morphologia Experimentia., new series* **6**:177-191.
- Stanisstreet, M., Wakely, J. and England, M.A. (1980). Scanning electron microscopy of wound healing in *Xenopus* and chick embryos. *Journal of Embryology and Experimental Morphology* **59**:341-353.
- Strome, S. (1993). Determination of cleavage planes. *Cell* **72**:3-6.
- Takahashi, H. (1988). changes in peanut lectin binding sites on the neuroectoderm during neural tube formation in the bantam chick embryo. *Anatomy and Embryology* **51**:49-62.
- Trelstad, R.L. Hay, E.D. and Revel, J-P. (1967). Cell contact during early morphogenesis in the chick embryo. *Developmental Biology* **16**:78-106.
- Van Straaten, H.W.M., Hekking, J.W.M., Consten, C. and Copp, A.J. (1993). Intrinsic and extrinsic factors in the mechanism of neurulation: effect of curvature of body axis on closure of the posterior neuropore. *Development* **117**:1163-1172.

- Waterman, R.E. (1975). SEM observations of surface alterations associated with neural tube closure in the mouse and hamster. *The Anatomical Record* **183**:95-98.
- Waterman, R.E. (1976). Topographical changes along the neural folds associated with Neurulation in the hamster and mouse. *American Journal of Anatomy* **146**:151-172.
- Whitby, D.J. and Ferguson, M.W.J. (1991a). The extracellular matrix of lip wounds in fetal, neonatal and adult mice. *Development* **112**:651-668.
- Whitby, D.J. and Ferguson, M. (1991b). immunohistochemical localization of growth factors on fetal wound healing. *Developmental Biology* **147**:207-215.
- Wyllie, A.H., Kerr, J.F.R. and Currie, A.R. (1980). Cell death: the significance of apoptosis. *International Review of Cytology* **68**:251-306.

APPENDIX

Salt solutions

0.9% Saline

9.0g of Sodium chloride was weighed. This was dissolved in 1000ml of freshly prepared distilled water.

Phosphate-buffered saline

8.5g of Sodium chloride, 0.85g of sodium phosphate, dibasic (Na_2HPO_4), and 0.54g of potassium phosphate, monobasic (KH_2PO_4) were weighed. The dry chemicals were then dissolved in 1000ml of freshly prepared distilled water.

Buffers

0.2M sodium cacodylate buffer solution

Solution A: 4.28g of sodium cacodylate powder ($\text{Na}(\text{CH}_3)_2\text{AsO}_2 \cdot 3\text{H}_2\text{O}$) was dissolved in 100ml distilled water to prepare 0.4M sodium cacodylate.

Solution B: 1 ml of concentrated hydrochloric acid (HCL) was diluted with 60.3 ml distilled water to prepare 0.2M HCL.

To prepare 0.2M sodium cacodylate buffer at pH 7.4, 8ml of solution B was added to 50ml of solution A, and the resulting solution diluted further with distilled water make volume up to 100ml.

Fixatives**2.0% paraformaldehyde, 2.0% glutaraldehyde in 0.1M sodium cacodylate buffer**

Solution A: 2.0g of powdered paraformaldehyde was dissolved in 20ml of double distilled water and heated to 60-65 °C in a fume cupboard to form 10% paraformaldehyde solution. Few drops of 1.0M sodium hydroxide was added until the solution becomes clear. It was then cooled before use.

Solution B: 10ml 2.5% glutaraldehyde solution was measured into a conical flask.

To prepare the fixative 50ml of 0.2M sodium cacodylate buffer is mixed with solutions A and B and topped to the 100ml with distilled water.

1.0% osmium tetroxide (cacodylate buffered)

A vial containing 1.0g solid osmium tetroxide was thoroughly washed to remove all traces of dirt. After drying, the vial was wrapped in a clean sheet of paper and broken. The paper and its content were put in a clean reagent bottle. 10ml of 0.2M sodium cacodylate buffer was added in a fume cupboard, shaken carefully and left overnight at 4 °C in a refrigerator to store. The pH of the solution was adjusted to 7.4.

DehydrationReagents

50%, 70% and 95% alcohol were prepared by making 50ml, 70ml and 95ml of absolute ethanol respectively up to 100ml with the required volumes of distilled water.

Dehydration schedule employed:

50% alcohol-----30 minutes
 70% alcohol-----2 hours
 95% alcohol-----30 minutes
 100% alcohol-----30 minutes

Preparation of embedding Resin (Embed 812)

Mixing Procedure:

Mixture A

Embed 812	5ml
DDSA	8ml

Mixture B

Embed 812	8ml
NMA	7ml

Final Embedding Mixture

Mixture A	13ml
Mixture B	15ml
DMP-30	16drops

Immediately before use, the two mixtures (A and B) were blended, and an accelerator (DMP-30) was added in a proportion of 1.5-2.0%. A teflon stirring rod was used during mixing to prevent the formation of air bubbles in the mixture.

Stains

1.0% toluidine blue stain

1.0g of toluidine blue was dissolved in 100ml of distilled water containing 1.0g of sodium tetraborate. The solution was filtered with a grade 1 filter paper and stored at room temperature.

Uranyl acetate

1.0g of uranyl acetate was added to 20ml of 50% alcohol in a bottle wrapped in aluminium foil. The mixture was stirred thoroughly with a magnetic stirrer until the uranyl acetate was completely dissolved. The solution was filtered with a millipore filter paper and stored at 4°C

Lead citrate

1.33g of lead nitrate ($\text{Pb}(\text{NO}_3)_2$) and 1.76g of sodium citrate were added to 30ml distilled water. The mixture was allowed to stand for 30 minutes with intermittent vigorous shaking till a milky solution was formed. 8.0ml of 0.1M sodium hydroxide (NaOH) was added, and the solution was made up to 50ml with distilled water.